Nanoscale

REVIEW

View Article Online
View Journal | View Issue

Check for updates

Cite this: *Nanoscale*, 2023, **15**, 8473

Anti-corrosion strategy to improve the stability of perovskite solar cells

Liang Li, Zhenyu Guo, Rundong Fan and Huanping Zhou *

Received 4th January 2023,
Accepted 19th March 2023

DOI: 10.1039/d3nr00051f

rsc.li/nanoscale

In recent years, perovskite solar cells (PSCs) have been considered as one of the most promising photovoltaic technologies due to their solution processing, cost effectiveness, and excellent performance. The highest certified power conversion efficiency (PCE) achieved to date is 25.8%, which is approaching the best PCE of 26.81% achieved for silicon-based cells. However, perovskite materials are susceptible to various aging stressors, such as humidity, oxygen, temperature, and electrical bias, which hinder the industrialization of perovskite photovoltaic technologies. In this review, we discuss the lifetime of PSCs from the perspective of corrosion science. On one hand, benefiting from a series of anti-corrosion strategies (passivation, surface coating, machining *etc.*) used in corrosion science, the stability of perovskite devices is remarkably enhanced; on the other hand, given that perovskites are soft crystal lattices, which are different from traditional metals, the revealed degradation processes and specific methods to improve device operation stability can be applied to the field of corrosion, which can enrich and expand corrosion science.

Published on 24 mars 2023. Downloaded on 22.06.2024 18.45.27.

1. Introduction

Materials science has shaped the development of civilizations since the dawn of mankind.[1–3] The birth of a new material will bring about profound changes in society and promote the progress of human civilization.[4,5] In recent years, metal halide perovskites have been a hotspot in semiconductor materials due to their excellent optoelectronic properties, easy processing capability, tunable bandgaps, and high tolerance to defects.[6–15] Perovskite solar cells (PSC) have shown remarkable progress in recent years with rapidly increasing power conversion efficiencies (PCEs) of up to 25.8%,[16] approaching that of the state-of-the-art PCE of 26.81% obtained for crystalline-silicon solar cells. However, metal halide perovskites (MHPs) can degrade when exposed to humidity, oxygen, temperature, electrical bias, illumination, and stress,[17–25] which hinders the commercialization of the resultant photovoltaic technology.[19,26]

The poor stability of perovskite devices is mainly associated with the degradation of the perovskite crystals upon exposure

Beijing Key Laboratory for Theory and Technology of Advanced Battery Materials, Key Laboratory of Polymer Chemistry and Physics of Ministry of Education, School of Materials Science and Engineering, Peking University, Beijing 100871, P. R. China. E-mail: happy_zhou@pku.edu.cn

Liang Li

Liang Li is currently a postdoctoral fellow in the School of Materials Science and Engineering, Peking University. He received his Ph.D. degree from the School of Metallurgy and Ecological Engineering, University of Science and Technology Beijing, in 2018. After that, he joined the Beijing Institute of Technology as a postdoctoral researcher from 2018 to 2020. His research interest is focused on perovskite-based photoelectric devices.

Zhenyu Guo

Zhenyu Guo received his B.S. degree in 2018 from the School of Materials Science and Engineering, Tianjin University. And now he is a Ph.D. candidate under the supervision of Prof. Huanping Zhou in the School of Materials Science and Engineering, Peking University. His current research interest is in developing high-efficiency and stable perovskite light-emitting diodes.

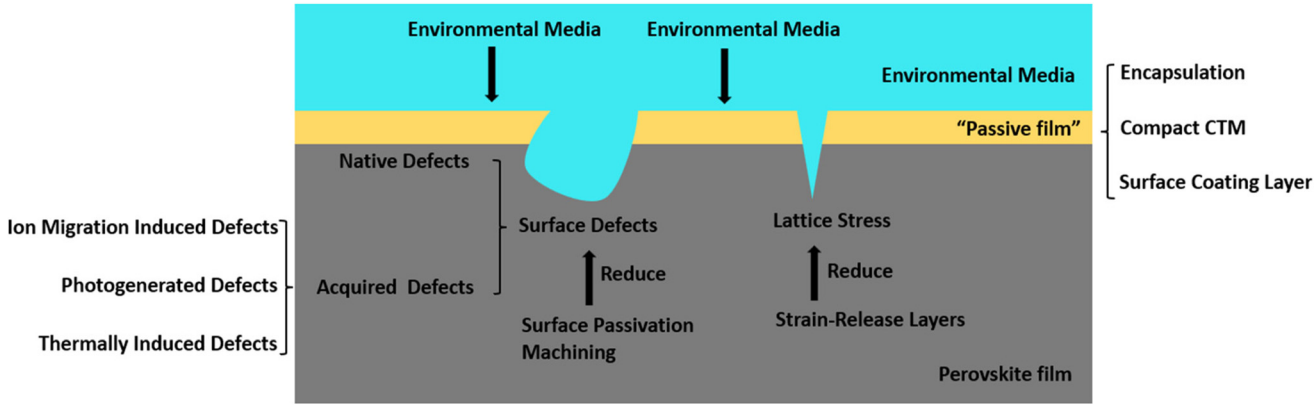

Fig. 1 Anti-corrosion strategies to improve the stability of perovskite solar cells.

Published on 24 mars 2023. Downloaded on 22.06.2024 18.45.27.

to various stressors.[19,27] Aging stressors can be divided into two categories: extrinsic and intrinsic.[28] The extrinsic stressors are affected by the interaction of the device with environmental species such as moisture and oxygen, and the intrinsic stressors include heat, illumination, and bias (independent of the protective environment or device packaging).[28] Among them, the adverse influence induced by extrinsic factors could be minimized by surface modification of the perovskite film and encapsulation on the perovskite devices.[28–30] The deterioration of perovskite materials could be simultaneously caused by intrinsic and extrinsic factors. These characteristics of perovskite material aging are in full compliance with the definition of material corrosion.[31] Before the 1960s, corrosion was usually defined as the degradation of metals through an electrochemical process.[32–34] Now, this concept is applicable to many other types of materials and is further defined as an attack on a material due to the electrochemical, chemical, and physical effects of the surrounding medium.[32] For example: plastic swelling or cracking, wood dry cracking or decay, wind erosion of granite, cement peeling off, *etc.* All the above-mentioned phenomena belong to the category of material corrosion.[32] So, we have learned from corrosion science and consider that perovskite corrosion refers to a perovskite material that has suffered from damage or degradation caused by chemical, electrochemical, and physical effects when exposed to environmental media (oxygen, humidity, light, electric field, *etc.*).[35]

Corrosion science can provide a range of strategies for enhancing the stability of perovskite materials (Fig. 1). In the case of corrosion, a medium is an element, compound, or solution that acts as a kind of condition for corrosion testing. During the aging process of perovskite solar cells, the corrosive medium refers to stressors including oxygen, humidity, light, heat, electric field, *etc.* A passive film, in terms of corrosion, refers to the spontaneous formation of an ultra-thin film of corrosion product on a metal's surface that acts as a barrier to additional chemical reaction. A passive film is very helpful in

Rundong Fan

Rundong Fan received his B.S. degree and Master's degree in 2014 and 2017, respectively, from the College of Engineering, Peking University. And now he is a Ph.D. candidate under the supervision of Prof. Huanping Zhou in the School of Materials Science and Engineering, Peking University. His research interest is focused on perovskite-based photoelectric devices.

Huanping Zhou

Huanping Zhou received her Ph.D. in inorganic chemistry from Peking University in 2010. Then, she joined the University of California, Los Angeles, as a postdoctoral researcher from 2010 to 2015. In July 2015, she joined Peking University as an assistant professor in the College of Engineering. Currently, she is a full professor in the School of Materials Science and Engineering, Peking University. She is a materials chemist with expertise in the fields of nanoscience, thin-film optoelectronics, organic/inorganic interface engineering, and the development and fabrication of related devices, such as photovoltaic cells, TFTs, and so on. Currently, her research lab is focused on thin-film optoelectronics, e.g., *perovskite materials and solar cells.*

This journal is © The Royal Society of Chemistry 2023

Published on 24 mars 2023. Downloaded on 22.06.2024 18.45.27.

mitigating corrosion damage. Degradation of the perovskite material can be prevented by coating the device with a surface coating, compact carrier transport material (CTM), and device encapsulation. The role of surface coating, compact CTM, and device encapsulation is similar to that of the passive film. It is generally believed that a well-formed passive film on a metal surface provides effective protection,[36] however, weak sites in the passive film can form at (i) grain boundaries, (ii) dislocations, (iii) flaws or mechanical damage, and (iv) nonmetallic inclusions or intermetallic compounds,[36] which thus become corrosion sites. For the perovskite materials themselves, the degradation process can be mitigated *via* the reduction of defects in the perovskite layer by various meaningful strategies, such as passivation,[37–42] machining[43–45] and stress relief,[46–48] because defects can serve as degradation initiation sites for the invasion of environmental media.

In this review, we discuss how anti-corrosion strategies used for traditional metals can enhance the stability of PSCs. We first introduce the defects that serve as the main degradation initiation sites for the invasion of environmental media. Then, the strategies designed to reduce defects during fabrication, including passivation, machining, and stress relief, are summarized and discussed with a particular emphasis on the effect of stress on PSC stability. In addition, it is particularly important to eliminate defects during device operation. Therefore, the newly emerging approaches used to eliminate defects during device operation are summarized. Subsequently, we review the strategies to prevent contact between corrosive media and the perovskites, including an interfacial layer, a carrier transport layer and the whole device design. Finally, we analyze the current challenges that PSCs still face and offer recommendations for stabilizing the perovskite devices.

2. Reducing corrosion sites to improve the stability of perovskite solar cells

From the perspective of corrosion sites, improving the crystalline quality of the perovskite films by passivation,[37–42] machining[43–45] and stress relief[46–48] can reduce the initial corrosion sites of the perovskite film, thereby increasing the operational lifetime of the perovskite solar cell. Passivation is a term from corrosion science often used for perovskite solar cells. Surface or bulk passivation of the perovskite leads to fewer corrosion sites, leading to improved perovskite solar cell stability. Machining, such as tape tearing and polishing, can remove the perovskite film surface corrosion sites, thereby improving the service life of perovskite solar cells. Stress compensation, such as the modification of negative thermal expansion polymer materials, successfully reduced the corrosion sites generated by stress cracking in perovskite films and reduced the aging rate of perovskite materials. However, the above-mentioned technical solutions for reducing perovskite corrosion sites based on anti-corrosion science can only reduce the defects generated during the preparation of perovskite films. In consideration of the fact that perovskites are soft crystal lattices, new defects are created during operation; this is rarely seen in conventional metal materials. Several *in situ* self-healing strategies have been developed to dynamically eliminate newly acquired defects generated during operation.

2.1. Passivation

Passivation is a common metal surface treatment process to protect against corrosion. Passivation creates a protective layer that does not easily chemically react with corrosive media and cause corrosion.[49,50] Passivated stainless steel prevents rust.[51] The perovskite thin films are usually prepared by a solution process, in which changing the structure and composition of the material from the precursor to the perovskite introduces various defects. According to different positions of passivation, passivation can be divided into top surface passivation,[52–54] bulk passivation[55,56] and buried interface passivation.[48,57–59] Among various types of passivation, surface passivation is a major way to achieve high performance and stable perovskite devices.[60] In the following, we concentrate on various types of surface passivators, such as non-halide salts, halide salts, and neutral molecules, which have been shown to facilitate the modification of perovskite surfaces and boost the lifetime of perovskite photovoltaics.

2.1.1. Non-halide salts. Stronger bonding between the perovskite surface and passivators is crucial to prevent degradation of the perovskite film. In 2019, Huang *et al.*[61] reported a typical passivation method to form a dense and thin $PbSO_4$ layer on the perovskite surface *via* an *in situ* reaction with selected inorganic anions (Fig. 2a). The resulting perovskite devices (encapsulated) retained 96.8% of the original PCE over 1200 h maximum power point (MPP) tracking under illumination in air (~60 ± 10% relative humidity (RH), ~65 °C), while reference devices maintained 46.9% of the original efficiency over 474 h.[61] This result indicates that the inorganic passivator has a superior effect on the passivation of defects. Fang *et al.*[62] reported a surface sulfidation treatment (SST) to build stable heterojunctions, resulting in SST devices retaining 91.8% of the original efficiency after 2200 h at 85 °C. Yang *et al.*[63] reported that tosylate (TsO^-) surface treatments resulted in a positive work function shift, resulting in a higher activation energy for ion migration, which maintained 88.5% of their original efficiency over 2092 h of operation.

2.1.2. Halide salts. Halide salts are commonly used as passivators for high performance and stable perovskite photovoltaics. In 2019, our research team found that organic cations and halide anion vacancies could be well passivated through adding trace amounts of fluoride to the perovskite precursor.[64] In 2022, Peng *et al.*[52] reported the introduction of 2-amidinopyrimidine hydrochloride into wet perovskite thin films to simultaneously regulate the charge traps and crystallization. The 2-amidinopyrimidine hydrochloride could not only compensate for formamidinium (FA) vacancies by forming hydrogen bonds with FAI, but also coordinated with undercoordinated

Published on 24 mars 2023. Downloaded on 22.06.2024 18.45.27.

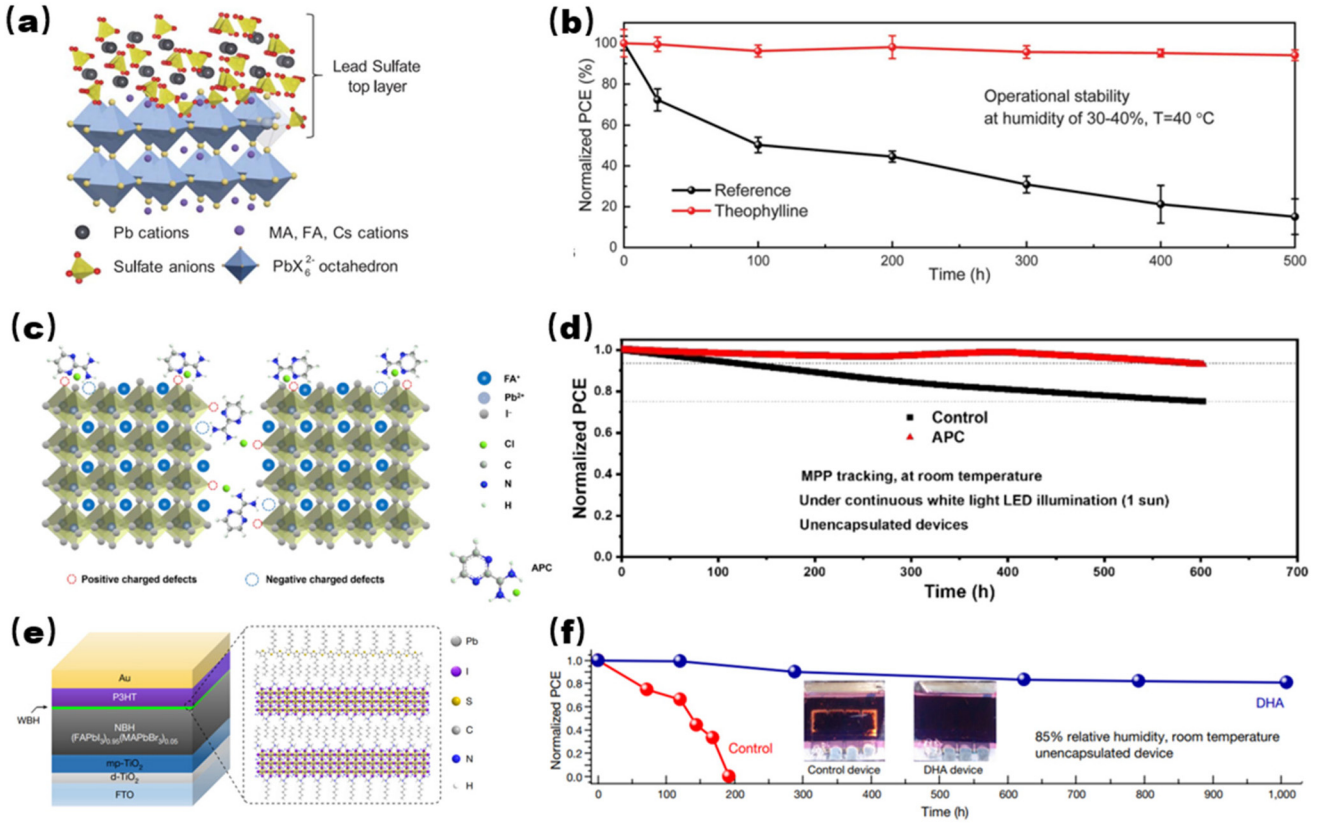

Fig. 2 (a) Schematic diagram of the protection of perovskites by *in situ* formation of a $PbSO_4$ top layer on the perovskite surface. Reproduced with permission.[61] Copyright 2019 Science. (b) Efficiency evolution measured for theophylline-treated or non-theophylline-treated packaged PSCs exposed to constant illumination (90 ± 10 mW cm^{-2}). Reproduced with permission.[60] Copyright 2019 Science. (c) Schematic diagram of the proposed interaction mechanism between 2-amidinopyrimidine hydrochloride and the perovskite.[52] (d) Dynamic MPP tracking of the unencapsulated 2-amidinopyrimidine hydrochloride treated and control devices under constant illumination. Reproduced with permission.[52] Copyright 2022 The Royal Society of Chemistry. (e) Left, structure of the PSC based on a double-layered halide architecture using P3HT as the HTM. Right, schematic diagram of the interface between the wide bandgap halide and P3HT.[76] (f) Results of humidity stability tests on the unsealed double-layered halide architecture and control devices under 85% RH at RT. Inset, photographs of the double-layered halide architecture (right) and the control (left) device after 200 h under 85% RH at RT. Reproduced with permission.[76] Copyright 2019 Nature.

Pb^{2+} (Fig. 2c), thereby inhibiting the formation of trap states for enhanced PSC stability. The resulting PSC retained 93% of the initial efficiency over 600 h of MPP operation under illumination (N_2 atmosphere, ~30 °C), whereas the reference PSC retained 75% of the initial efficiency over 600 h of MPP operation (Fig. 2d). Huang *et al.*[65] reported that quaternary ammonium halides could well passivate ionic defects with their positive-charged and negative-charged components. Zhao *et al.*[66] explored perovskite surface passivation with a range of phenylalkylammonium iodides with different alkyl chain lengths. The stabilizing effect increases with chain length because the perovskite surface is more strongly bound to the molecule. Tan *et al.*[67] developed 4-trifluoromethyl-phenylammonium (CF3-PA) passivated Pb–Sn perovskites, and the passivated tandem solar cells retained 90% of the initial PCE over 600 h of MPP operation and exhibited better operational stability than the control device.

It is generally considered that two-dimensional (2D) or quasi-two-dimensional (quasi-2D) perovskites can be formed on the surface using halide salts. 2D materials are commonly used as metal anticorrosive materials due to their advantages of not affecting the surface morphology of coatings.[68–75] In 2019, Seo *et al.*[76] introduced a double-layered halide architecture, in which an ultrathin wide bandgap perovskite was stacked on a narrow bandgap absorber before depositing the hole transport material (HTM) (Fig. 2e). The purpose of introducing the wide bandgap perovskite layer is to eliminate defects at the perovskite/poly(3-hexylthiophene) (P3HT) interface.[76] The $N^+(CH_3)_3^-$ moiety was reported to form a perovskite surface that resisted degradation under wet conditions.[77] The PSC (unencapsulated) with double-layered halide architecture retained ~80% of the original PCE over 1008 h under 85% RH at room temperature (RT), whereas the control device completely decayed within 200 h (Fig. 2f).[76] De Wolf *et al.*[78] fabricated perovskite devices through tuning the dimensional fragments of 2D perovskite formed with oleyl ammonium iodide at RT. The treatment inverted perovskite devices deliver 24.3% efficiency and retain >95% of the original efficiency for more

 This journal is © The Royal Society of Chemistry 2023

Published on 24 mars 2023. Downloaded on 22.06.2024 18.45.27.

than 1000 h under damp heat test conditions. Furthermore, 2D perovskites refer not only to Ruddlesden-Popper perovskites (RP), but also to Dion-Jacobson (DJ) perovskites formed with divalent organoammonium cations. Zhu *et al.*[79] reported that *N*,*N*-dimethyl-1,3-propane diammonium ($DMePDA^{2+}$) treatment to form a 2D DJ phase thin layer was the usual strategy to enhance the device PCE and stability. The $DMePDAI_2$-modified device retained 90% of its original efficiency over 1000 h of operation, while the efficiency of the reference device dropped by 43%. Some inorganic halides can also form 2D structures. Loo *et al.*[80] deposited a fully inorganic $Cs_2PbI_2Cl_2$ 2D perovskite by treating the surface of the $CsPbI_3$ film with a CsCl solution. The $Cs_2PbI_2Cl_2$ capping device retained 80% of the original PCE after annealing at 110 °C under constant illumination for 2100 hours.

2.1.3. Neutral molecules. The most common defects in perovskite materials are charge point defects, which can be passivated *via* Lewis acids or bases. Some organic neutral molecules with charged functional groups can reduce defects. In 2019, Yang *et al.*[60] reported that through utilizing theobromine, caffeine and theophylline as surface passivators, Pb_I antisite defects were well passivated. Studies have shown that theophylline is the most effective at passivation. The theophylline treated devices (packaged) achieved the highest efficiency of 23.48% along with a long lifetime: it retained >95% of the original PCE over 500 h under constant illumination (30–40% RH, ~40 °C), while the control devices retained 20% of the original PCE over 500 h under the same conditions (Fig. 2b). Han *et al.*[81] constructed strong Pb–O and Pb–Cl chemical bonds by deposition of Cl–GO, resulting in PSCs with 90% retention of their original efficiency over 1000 h of operation. Additionally, Li *et al.*[82] introduced a sesquiterpene lactone named artemisinin into perovskite films to increase the V_{OC} and then the performance of flexible devices, resulting in flexible perovskite devices with better long-term stability and mechanical stability.

2.2. Machining

Machining is an effective method of corrosion protection. Uddin *et al.*[83] reported that the improved surface integrity resulting from machining could enhance the corrosion resistance of a Mg-based alloy when compared to the original unprocessed surface. A similar study appears in the field of PSCs. The ionic properties of the perovskite lead to a large number of charged surface defects under high temperature annealing, while reducing surface defects is crucial for boosting the lifetime of the perovskite photovoltaics. However, the main defects are distributed on the perovskite surface, so reducing the defects on the perovskite surface is key to enhancing the lifetime of the perovskite photovoltaics. In 2020, Huang *et al.*[43] reported a strategy to remove the defective perovskite with adhesive tape without affecting the underlying crystalline regions.[81,84,85] Tapes made of soft adhesive on a flexible polymer substrate are pressed onto the rough and defective perovskite film surfaces to form an intimate contact with an appropriate bonding strength (Fig. 3a).[43] Tape treatment was carried out by pressing low-cost 3M Temflex 1700[86] tape onto $MAPbI_3$ ($MA = CH_3NH_3$) films and then detaching the tape from the perovskite surfaces, as schematically illustrated in Fig. 3a.[43] The right half of the sample, which had undergone tape treatment, remained black after 8 hours of illumination, while the left half had degraded to yellow phases in <4 h, indicating that tape treatment could enhance the photostability of the film (Fig. 3b). The enhanced film photostability is thanks to the removal of defective surface layers. The efficiency of a sealed reference PSC decayed quickly from 19.1% to 14.7% over 324 h (Fig. 3g). In contrast, the tape treated PSCs retained 97.1% of the initial efficiency after 1440 h of illumination. This simple machining strategy, tape treatment, remarkably increased the photostability of PSCs *via* removing defective surface layers. In 2021, Huang *et al.*[44] reported that some amorphous phases and nanocrystals were observed on the surface of polycrystalline films deposited by a solution deposition method, which accelerated the decomposition of the perovskite. The lifetime of the perovskite films is remarkably enhanced by polishing to remove the amorphous phase and nanocrystalline layers.[44] They tested the photostability of $MAPbI_3$ films with different polishing depths. In order to avoid the influence of morphology changes of the perovskite film on the stability, only half of each perovskite film was polished. It is found that the perovskite decomposes to lead iodide and other species, under light soaking in ambient air, causing de-colorization of the films.[21,87,88] The films polished to remove 96 nm and 118 nm exhibited better photostability than films polished to remove 42 nm (Fig. 3c–f).[44] All of these reports highlight that machining is a useful strategy to reduce surface defects, which can be further developed for more robust devices.

2.3. Stress relief

Stress relief is an effective way to eliminate stress corrosion. Stress corrosion is a kind of corrosion that occurs due to the simultaneous action of a corrosive medium and sustained tensile stress.[89] Undesirable strain in the perovskite film during film fabrication refers to extension/narrowing of chemical bonds and expansion/contraction of the lattice volume, which affects the lifetime of devices.[90] Strain engineering has been developed as a novel strategy to improve the efficiency and lifetime of PSCs.[91] In 2020, Sargent *et al.*[92] compensated for residual tensile strain through introducing an external compressive strain from the hole transport layer (HTL). Residual tensile strain in the perovskite films originates from the thermal expansion coefficient mismatch between substrates and perovskites. The thermal expansion coefficient of each functional layer material varies greatly (Fig. 4a).[92] The commonly used ITO glass and inorganic charge transport layers have low values of α ranging from 0.37 to 1×10^{-5} K^{-1}.[93] In contrast, perovskites possess much higher α values in the range of 3.3 to 8.4×10^{-5} K^{-1},[94–96] about 10 times higher than that of the electron transport layers (ETLs) or substrates. Such a large difference in the thermal expansion coefficient is the main reason for tensile strain in the perovskite films when it is

Published on 24 mars 2023. Downloaded on 22.06.2024 18.45.27.

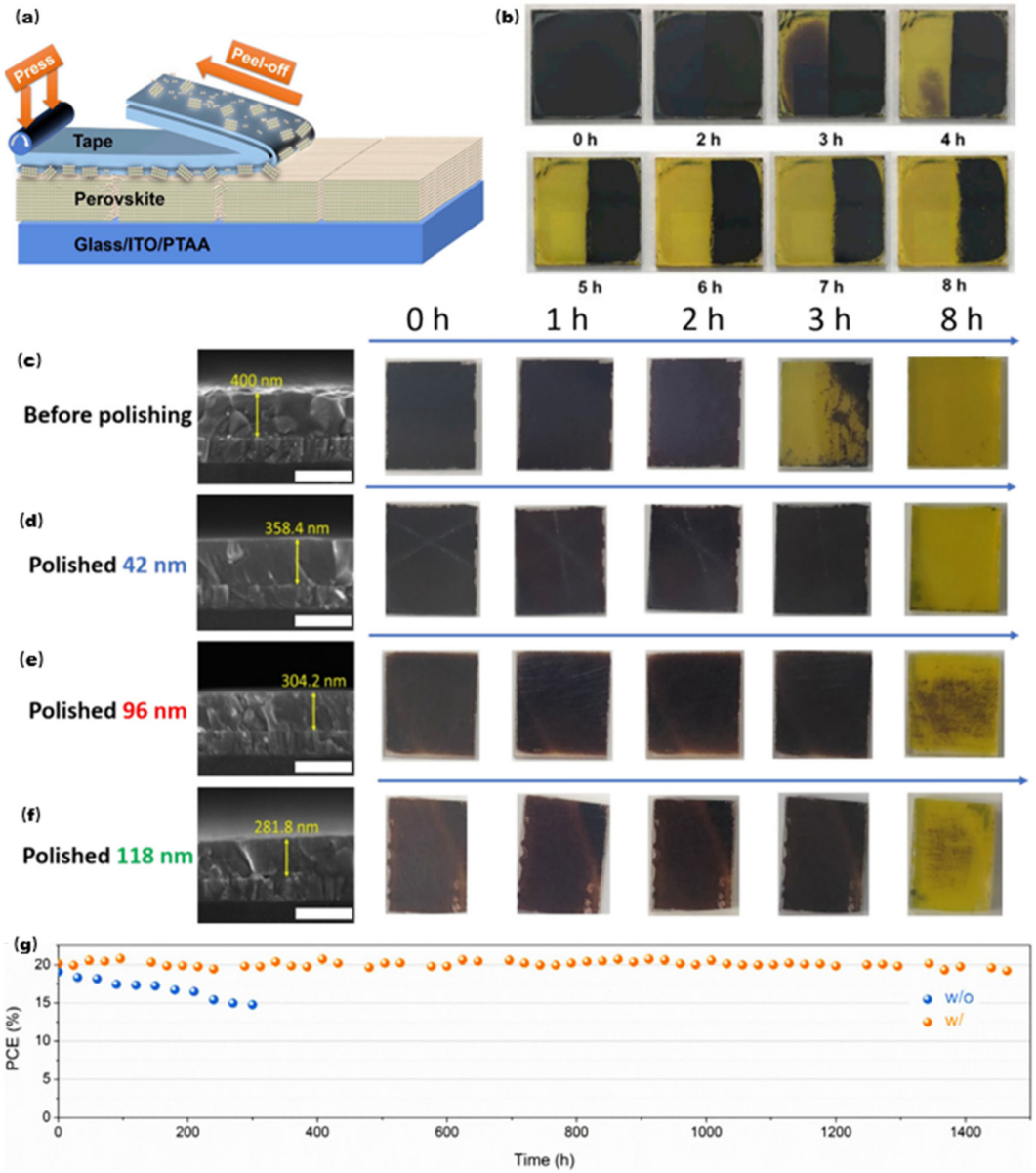

Fig. 3 (a) Schematic of peeling adhesive tape off a perovskite film.[43] (b) Optical image of a perovskite film, with an area of 15 mm × 15 mm prepared by a one-step method, after illumination for different time intervals. The right part of the film was tape treated.[43] Optical images of the perovskite films in a glass stability test with different polishing depths by polishing-off layer-by-layer: (c) initial thickness of 400 nm, (d) polished-off 42 nm, (e) polished-off 96 nm, (f) polished-off 118 nm. Their cross-section SEM images are shown in the left column, and the scale bar inside is 500 nm. Reproduced with permission.[44] Copyright 2021 The Royal Society of Chemistry. Same illumination as previous tests in ambient air. (g) Operational stability of sealed solar cells based on $Rb_{0.05}Cs_{0.05}FA_{0.85}MA_{0.05}PbI_{2.85}Br_{0.15}$ perovskite layers with and without tape treatment. Reproduced with permission.[43] Copyright 2020 Elsevier Inc.

cooled to RT.[97,98] When a perovskite layer is deposited on a substrate with lower α, the contact formed between the two layers during the high temperature annealing process limits the shrinkage of the perovskite upon cooling to RT, thereby introducing tensile strain in the in-plane direction (Fig. 4b).[92] The evolution of the efficiency of the perovskite devices was similar to the case under MPP conditions (Fig. 4c).[92] The tensile-strained PSC lost a great deal of efficiency, whereas the compressive-strained and non-strained PSCs retained 96% and 80% of the original PCE over 1000 hours of heating at 85 °C. This work highlights the importance of strain-free perovskites on the stability of devices, because strain causes an increase in defects which serve as degradation initiation sites under real operational conditions.

To further relieve stress, changing the expansion coefficient of the perovskite materials is a strategy to release stress from the perovskite materials. Chen *et al.*[99] reported the elimination of residual stress in perovskite films through introducing

 This journal is © The Royal Society of Chemistry 2023

Published on 24 mars 2023. Downloaded on 22.06.2024 18.45.27.

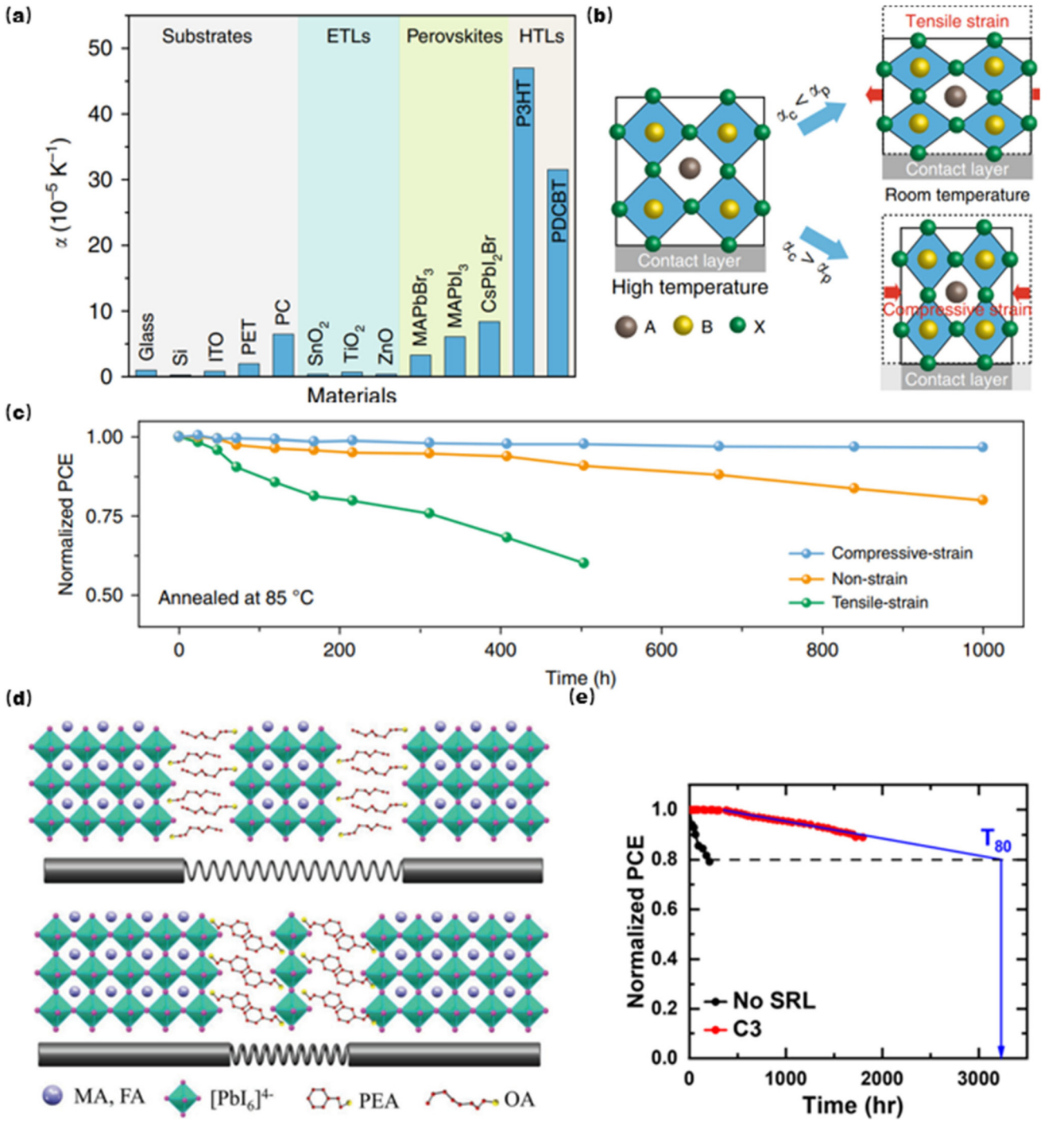

Fig. 4 (a) Thermal expansion coefficients of commonly used materials in the perovskite devices.[92] (b) Schematic showing the formation of tensile and compressive strains.[92] (c) Normalized evolution of the efficiency of the perovskite devices maintained at 85 °C under a N_2 atmosphere. Reproduced with permission.[92] Copyright 2020 Nature. (d) Schematic describing residual stress relief with soft and stiff structural subunits. Reproduced with permission.[99] Copyright 2019 Wiley-VCH GmbH. (e) Evolution of normalized efficiency for sealed $CsPbI_3$-based devices without strain-release layers and that with C3 strain-release layers. The devices were aged at the MPP under 1-sun illumination under ambient conditions (~40 °C, ~40% RH), in accordance with the ISOS-L-1I protocol. Reproduced with permission.[100] Copyright 2022 American Chemical Society.

different A-site cations. Since the two-dimensional perovskite composition is formed after this treatment, residual stress in the perovskite film can be effectively released to approximately 50%.[99] The mixed 2D/3D structure resembles a "bone-joint" (Fig. 4d), which enhances the stability of PSCs against external light/thermal stresses through a cushioning effect.

Published on 24 mars 2023. Downloaded on 22.06.2024 18.45.27.

Furthermore, Loo *et al.*[100] introduced alkyltrimethoxysilane strain-release layers (SRLs) at the perovskite/substrate interface. The resulting devices were aged at the MPP under illumination according to ISOS-L-1I.[28] The butyltrimethoxysilane treated solar cells retained >90% of the initial PCE after 1798 h, while the strain-release layer free PSCs retained 80% of the original PCE after 209 h under the same conditions as shown in Fig. 4e.[100]

2.4. Self-healing

The strategies introduced above to improve the operational lifetime of PSCs, such as passivation, machining, and stress relief, are all achieved by reducing the defects generated during the preparation of the perovskite films. However, the perovskite materials are soft lattices. During the operation of PSCs, heat, light and bias voltage will induce new defects, which are also the initiation sites for the degradation of the perovskite materials. Some studies have reported that I^- in perovskites can be prone to being oxidized to I^0, which not only acts as a carrier recombination center, but also triggers chemical chain reactions to accelerate the decomposition of PSCs.[21] Furthermore, Pb^{2+} is easily reduced to metallic Pb^0 upon illumination or heating, as observed in lead-based halide perovskite films.[20,101] Metallic Pb^0 is a dominant deep defect state that seriously degrades the photovoltaic performance of PSCs.[102,103] Most importantly, all of these defects (I^0 and Pb^0) generated during the operation of PSCs also adversely affect the operational lifetime of the perovskite devices. In 2019, our research team proposed a "redox shuttle", which independently reduced I^0 and oxidized Pb^0, through using the Eu^{3+}–Eu^{2+} ion pair according to the following chemical reactions: $Eu^{2+} + I^0 \rightarrow Eu^{3+} + I^-$; $2Eu^{3+} + Pb^0 \rightarrow 2Eu^{2+} + Pb^{2+}$ (Fig. 5a).[104] Interestingly, the Eu^{3+}–Eu^{2+} ion pair was not consumed during PSC operation, which might be due to it having a suitable redox potential and its nonvolatility in this cyclic transition. Repairing Pb^0 and I^0 defects using a redox shuttle proved to be effective, and the dynamic passivation method should be further developed for more operationally stable perovskite devices. The freely moving halogen ions and generation of photoinduced defects are dynamically updated. Accordingly, most methods are short-term and static, which make enhancements in light stability very limited. Therefore, there is an urgent need to find new passivation methods to match the defects generated during device operation. In 2022, Song *et al.*[105] proposed a tautomeric passivation approach for molecular isomerism passivation to assist defect passivation for light stable perovskite devices with sustainable ultraviolet (UV) protection. 2,3-Bis(2,4,5-trimethyl-3-thienyl) maleimide (DAE) helps passivate defects and enhances the photostability of devices, especially sustainable UV protection for devices (Fig. 5b).[105] DAE ($C_{18}H_{19}NO_2S_2$), through molecular isomerism, can repeatedly invert between open and closed-ring isomers, reaching kinetic equilibrium states (state I and state II) *via* absorbing UV (365 nm) and visible light (>500 nm), and sustaining UV on/off cycling in the precursor solution, and thus, it is capable of providing long-term light stable and sustainable UV protection to devices.[105] Later, Wang *et al.*[106] developed a sustainable dynamic passivation method for PSCs by adopting the photoisomeric molecule spiropyran. Our group[107] monitored the reversible phase-transition process of FA-dominated perovskites, namely δ-to-α phase (heat healing) and α-to-δ phase (humidity aging). The decayed PSCs were found to be healed after heating (Fig. 5c). This finding presents a feasible strategy to stabilize the α phase of FA-based perovskites and PSCs.

3. Minimizing the contact between perovskite solar cells and corrosive medium

According to the anti-corrosion strategy, on one hand, we should improve the crystal quality of the perovskite to reduce corrosion sites, on the other hand, we need to prevent contact between corrosive media and the perovskite to improve the stability of the perovskite solar cells. Besides, we also need to prevent contact between the corrosion medium and the perovskite, with respect to the interfacial layer, the carrier transport layer and the whole device. Firstly, a thin barrier shield may better protect the perovskite surface from corrosive media. Secondly, additive-free carrier transport materials could minimize contact between the perovskite film and the corrosive medium. Finally, by encapsulating the perovskite device, contact with the perovskite film could be effectively prevented, thus reducing the aging rate of the perovskite materials.

3.1. Surface coating

Most metals and their alloys, such as magnesium, nickel, copper, and carbon steel, are frequently subject to corrosion during industrial production. Anti-corrosion coatings can reduce the risk of corrosion by isolating metals from corrosive media. Covering metal surfaces with anti-corrosion coatings is a cost-effective strategy to prevent corrosion.[108] Since the perovskite surface is also susceptible to environmental stressors such as humidity, introducing some hydrophobic or hygroscopic molecules is an effective strategy to improve the operational lifetime of the perovskite devices. For hydrophobic molecules, previous studies by our group have shown that the amino group (NH_2-POSS) could effectively decrease the charge trap density of the perovskite and improve the humidity stability of the perovskite device.[109,110] In 2018, Saliba *et al.*[111] investigated the top interface between the hole transport layer and the perovskite using a poly(methyl methacrylate) (PMMA) layer on PSCs that already had a [6,6]-phenyl-C61-butyric acid methyl ester (PCBM):PMMA polymer mix at the electron transport layer interface (Fig. 6a). The polymer-modified device retained 93.4% of its original efficiency over 1000 h MPP operation under illumination (N_2 atmosphere), whereas control PSCs retained 78.35% of the initial efficiency over 1000 h under the same conditions (Fig. 6b). All of these results lead to

 This journal is © The Royal Society of Chemistry 2023

Published on 24 mars 2023. Downloaded on 22.06.2024 18.45.27.

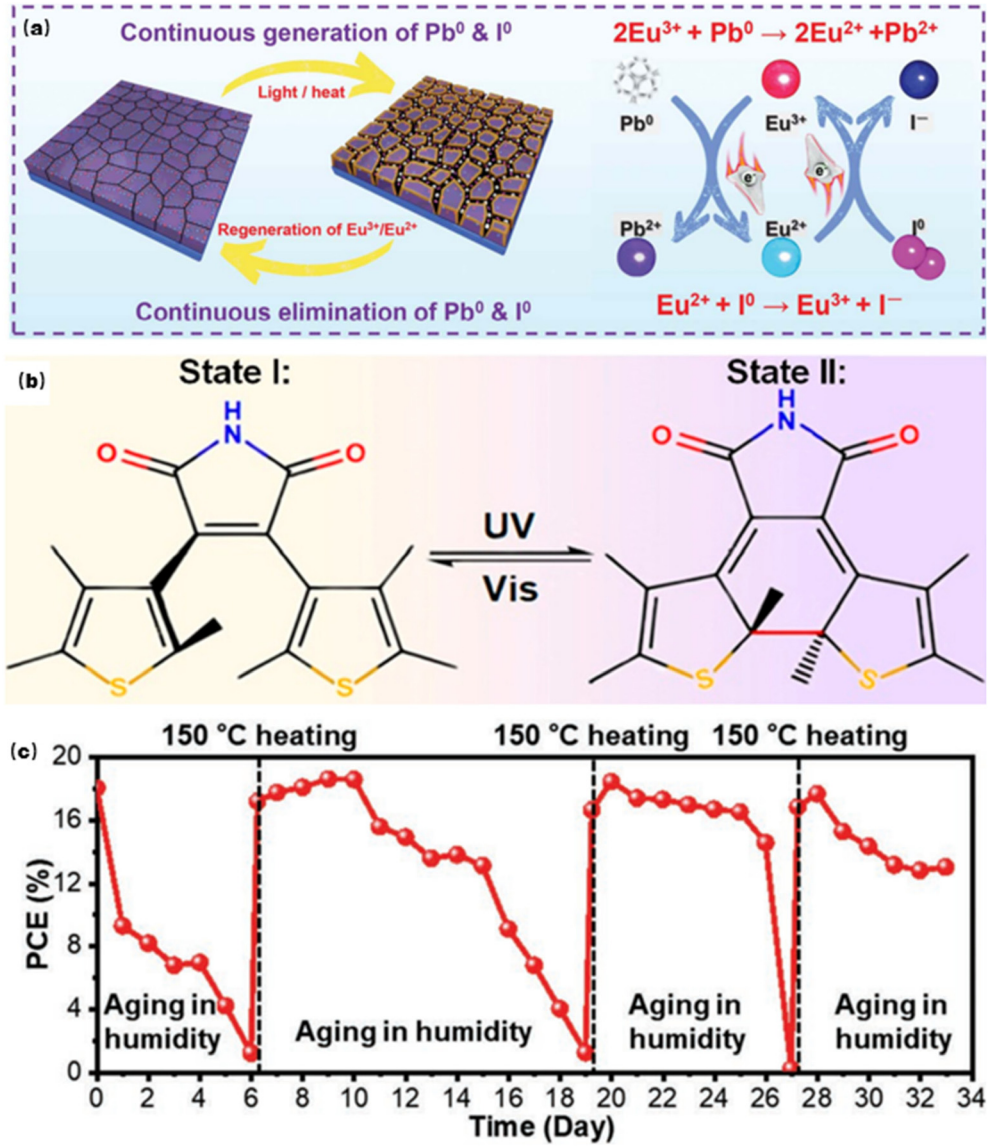

Fig. 5 (a) Illustration of the proposed mechanism of cyclic elimination of I^0 and Pb^0 defects and regeneration of the Eu^{3+}–Eu^{2+} metal ion pair. Reproduced with permission.[104] Copyright 2019 Science. (b) Diagram of a tautomeric DAE molecule with a dynamic nature (state I to state II). Reproduced with permission.[105] Copyright 2022 The Royal Society of Chemistry. (c) Performance healing of the aged devices by heating treatment. PCE of the same PSC during three cycles of "humidity aging–heat healing." Reproduced with permission.[107] Copyright 2022 Wiley-VCH GmbH.

a general method to enhance the moisture stability of perovskite devices, which not only have electron accepter or donor groups to passivate surface defects, but also have hydrophobic groups to prevent water intrusion.

Another class of molecules are hygroscopic polymers. In 2018, Petrozza *et al.*[112] selected two polymers with different moisture compatibilities, hygroscopic polyethylene oxide (PEO) and hydrophobic polystyrene (PS) (Fig. 6c). The PEO layer greatly slowed down the perovskite hydration process *via* absorbing moisture before invading the perovskites, thereby strongly enhancing the moisture stability of the corresponding perovskite films and devices. The PEO-based devices (unpackaged) maintained ~100% of their initial PCE after 14 h MPP operation under illumination under ambient conditions (50% RH), whereas control devices retained 75% of the original PCE over 14 h under the same conditions (Fig. 6d). Photographs of the degrading perovskite films were taken at 88% RH over 15 days (Fig. 6e). The black color of the perovskite film becomes transparent, indicating the transition of the perovskite to the hydrated phase.[10] For the as-received $MAPbI_3$ film without treatment, it is seen that transparent parts appear on the second day, and then gradually grow into large pieces. The number of transparent sites increases during hydration across the surface. The PS-treated perovskite film also exhibited transparent small spots on the third day that continued to grow. Compared with $MAPbI_3$, PS–$MAPbI_3$ has a lower number of

Published on 24 mars 2023. Downloaded on 22.06.2024 18.45.27.

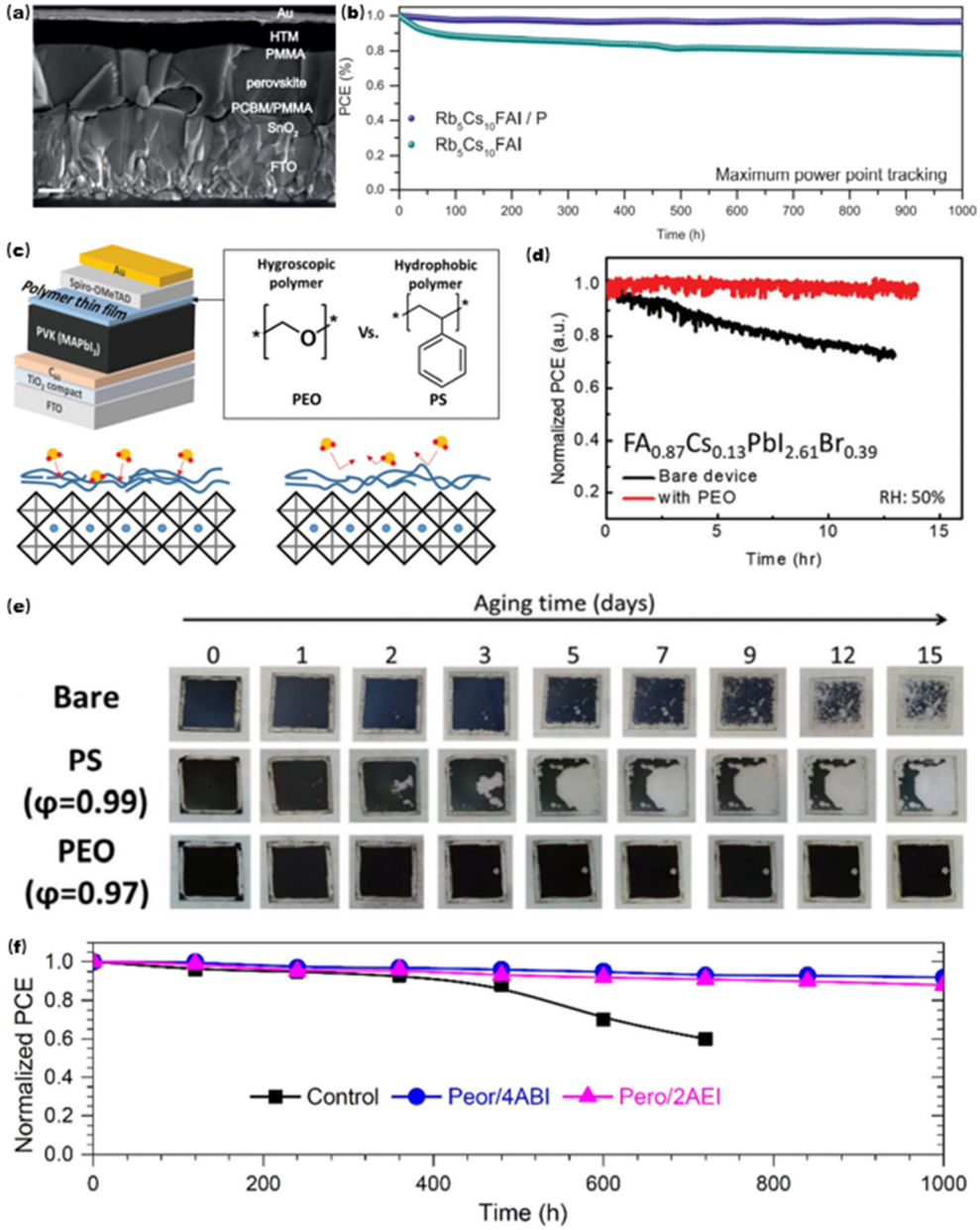

Fig. 6 (a) SEM image of a $Rb_5Cs_{10}FAPbI_3$ PSC with polymer layers consisting of PMMA at the perovskite/HTM interface and PCBM/PMMA at the SnO_2/perovskite interface.[111] (b) Stability of the $Rb_5Cs_{10}FAPbI_3$ PSC without polymer modification (green curve) and with polymer layers (blue curve) aged at RT over 1000 h of MPP operation under a N_2 atmosphere. Reproduced with permission.[111] Copyright 2018 Science. (c) The device structure of a PSC with polymers with chemical structures of PEO and PS and a schematic illustration of a polymer thin film assembled on the perovskite structure.[112] (d) Evolution of the efficiency of $FA_{0.87}Cs_{0.13}Pb(I_{0.87}Br_{0.13})_3$ PSCs without and with PEO, measured under AM 1.5, 100 mW cm^{-2} equivalent irradiance in air (~50 RH%).[112] (e) Optical images of the $MAPbI_3$ films with and without PEO and PS passivation layers processed from 10 mg ml^{-1} concentrations ($\psi > 0.98$) during exposure to 88% RH over two weeks. Reproduced with permission.[112] Copyright 2018 The Royal Society of Chemistry. (f) Stability tests for the perovskite devices stored under ~20% RH. Reproduced with permission.[113] Copyright 2020 American Chemical Society.

original nucleation sites that initiate hydration and decomposition, but they are all significantly degraded by the 15th day of exposure. On the other hand, the PEO-treated perovskite films exhibit completely different behavior from the pristine and PS-treated perovskite films. The perovskite film with PEO treatment did not change in appearance even over two weeks. In 2020, Park *et al.*[113] reported a new way to enhance the lifetime of the perovskite through utilizing the hydrophilic materials 4-amino-1-butanol hydroiodide (4ABI) and 2-aminoethanol hydroiodide (2AEI), which absorbed water molecules, and therefore, the perovskite could avoid a direct interaction with moisture. The efficiency of the reference device decreased

 This journal is © The Royal Society of Chemistry 2023

Published on 24 mars 2023. Downloaded on 22.06.2024 18.45.27.

to nearly 60% of its initial efficiency over 700 h, while both the 2AEI- and 4ABI-treated PSCs retained 90% of the original value over 1000 h (Fig. 6f). Using hygroscopic materials to take up moisture and passivate surface defects is another effective way to extend the lifetime of the perovskite devices; this approach needs further development.

3.2. Compact CTM

The anti-corrosion coating generally forms a barrier between the metal surface and corrosive medium. A thick shielding layer can better protect the perovskite from the intrusion of corrosive media. A compact carrier transport material provides the perovskites with a thick barrier shield that helps to retard the penetration of the corrosive medium through the carrier transport material. Usually in the n–i–p device architecture, the hole transport material is deposited on the perovskite surface. The lifetime of the perovskite devices is closely related to the additives, hydrophilicity and compactness of the hole transport materials.

Additives used to increase mobility in the HTM have hygroscopic and deliquescence properties, which attract water molecules and result in accelerated degradation of PSCs. In addition, the introduction of metal-salt additives would lead to additional pinholes in the HTLs due to the incompatibility between organic HTM molecules and metal-salt additives.[116] In 2017, Kim *et al.*[114] investigated the effects of additives in the HTM layer on the perovskite layer by neatly delaminating the interface between the HTM and perovskite layers. The accumulated additives accelerate the degradation of PSCs *via* decreasing the fracture energies and attracting moisture to the interface between the perovskite and HTM layers. In the HTL without additives (Fig. 7a), pinholes were present on the HTL surface. In that situation, degradation was concentrated on the HTL in the PSC, rather than over the entire film. However, when the (trifluoromethane) sulfonimide (Li-TFSI) additives were added to the HTM, the additives accumulated at the bottom along the thickness of the HTM as shown in Fig. 7b. The dispersed additives in the HTL attract moisture *via* the pinholes; thus, the stability of the entire HTL is low. In this case, moisture attacks the interface between the HTL and perovskite layer due to the large number of additives at the bottom of the HTL. Therefore, the perovskite layer is directly exposed to wet conditions and water molecules react with the perovskite. The HTM with additives had more pinholes on the surfaces as shown by the red circles in Fig. 7c. The additives remarkably accelerated the degradation of the pristine perovskite/HTM structure and this phenomenon became more severe with increasing exposure time. The fracture energies decreased significantly for the samples with the addition of ionic additives. Through adding the additives, the fracture energies of P3HT and 2,2′,7,7′-tetrakis(*N*,*N*-di-*p*-methoxyphenyl amino)-9,9′-spirobifluorene (Spiro-OMeTAD) decreased to 1.76 ± 0.4 J m^{-2} and 0.65 ± 0.21 J m^{-2}, respectively, from 5.07 ± 0.17 J m^{-2} and 1.61 ± 0.3 J m^{-2}, respectively. Although spiro-OMeTAD had weak adhesion due to its small molecule nature, the fracture energy remarkably decreased to below 1 J m^{-2} (Fig. 7d). Values lower than 1 J m^{-2} are reported to correspond to weak van der Waals interactions with no chemical bonding.[117] Therefore, fracture energies less than 1 J m^{-2} are too weak to withstand the pressure generated during degradation and the transition of water molecules from solid to gas; thus, delamination occurs at the interface. However, for P3HT, it is believed that even though additives remarkably reduce the interfacial fracture energy, the adhesion is sufficient to prevent large-scale delamination by disrupting additional crack propagation despite localized domain delamination. Thus, P3HT was considered to be a more promising HTM for perovskite device commercialization than spiro-OMeTAD. In 2021, Noh *et al.*[115] developed an efficient method to directly incorporate gallium (III) acetylacetonate ($Ga(acac)_3$) into P3HT without subsequent processes and hygroscopic dopants. The P3HT mixed with Ga $(acac)_3$ (GA-P3HT) PSC device retained 99% of its original efficiency over 2000 h under 85% RH at RT without encapsulation, while the reference device suffered severe PCE deterioration compared to the original efficiency (Fig. 7e).[115]

3.3. Encapsulation

When a metal is exposed to oxygen and moisture, it breaks down and corrodes. To prevent this from happening, encapsulation is a commonly used approach. Encapsulation is also an effective strategy to mitigate PSC degradation. In 2018, McGehee *et al.*[118] reported a glass-to-glass encapsulation method for perovskite devices that enabled them to pass the industry standard IEC 61646 damp heat and thermal cycling tests. Fig. 8a shows a side view of first-generation encapsulation. This design used soldered metal ribbons and evaporated metal fingers to conduct current from the device to the outside. Both edges of the ribbon were covered with a seal to minimize water molecule access. Additionally, the 2 cm × 2 cm device substrates were encapsulated in two pieces of glass and ethylene vinyl acetate (EVA) encapsulant. The first-generation encapsulation procedure enabled two perovskite devices to pass the IEC 61646 1000 h damp heat test. In the second-generation package, a transparent glass/indium doped tin oxide (ITO) electrode was used to separate the perovskite from the metal and ensure that there was 2 mm of lateral space between the evaporated metal and the devices (Fig. 8b). In the second-generation package, devices and electrical feedthroughs are located directly to one side of the glass cover to minimize water molecule access and reduce cavities created by device movement. In addition to high thermal stability, this polyurethane film-based encapsulation process can be easily scaled up to large-scale applications. Printable perovskite solar submodules with a size of 10 cm × 10 cm were fabricated as encapsulated devices using the same protocol, as shown in Fig. 8c.

In 2015, Weerasinghe *et al.*[120] presented the effect of encapsulation on enhancing the lifetime of flexible PSCs. The two encapsulation architectures adopted are illustrated in Fig. 8d and e. For the 'partially' packaged PSCs the electrical contacts are in direct contact with the PSCs, while for the 'completely' packaged PSCs the electrical connection is made through thin

Published on 24 mars 2023. Downloaded on 22.06.2024 18.45.27.

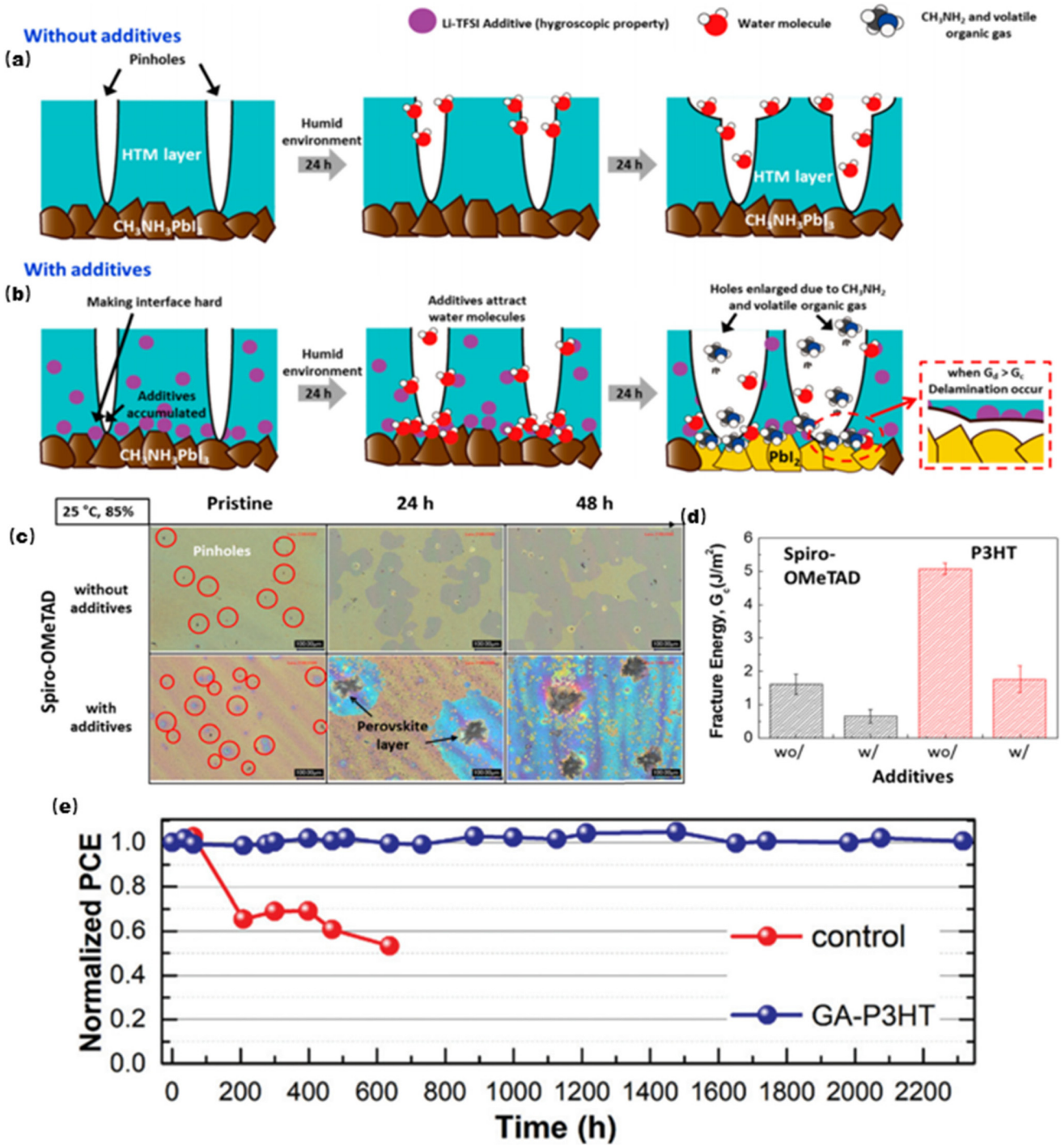

Fig. 7 Degradation mechanism of PSCs in humid environments (a) without additives and (b) with additives.[114] (c) Photographs of the spiro-OMeTAD specimens with and without additives obtained for the pristine sample and samples after 24 h exposure and 48 h exposure to 85% RH at 25 °C.[114] (d) Measured fracture energies of the spiro-OMeTAD and P3HT samples with and without additive addition before exposure to humid conditions. Reproduced with permission.[114] Copyright 2017 American Chemical Society. (e) Evolution of PCEs for humidity stability tests of PSCs under 85% RH at RT. The PSCs were tested without encapsulation. Reproduced with permission.[115] Copyright 2021 The Royal Society of Chemistry.

copper wires soldered to the modules. The PSC efficiency was measured before and after encapsulation, and packaged PSCs showed no noticeable change in PCE due to the lamination process. In 2019, Chen *et al.*[121] demonstrated the advantages of a low-temperature and solvent-free processing packaging method for the perovskite device, as well as the advantages of a cost-effective encapsulation material, paraffin. The thermal and humidity stability of the UV-curable adhesive (UVCA) with/

 This journal is © The Royal Society of Chemistry 2023

Published on 24 mars 2023. Downloaded on 22.06.2024 18.45.27.

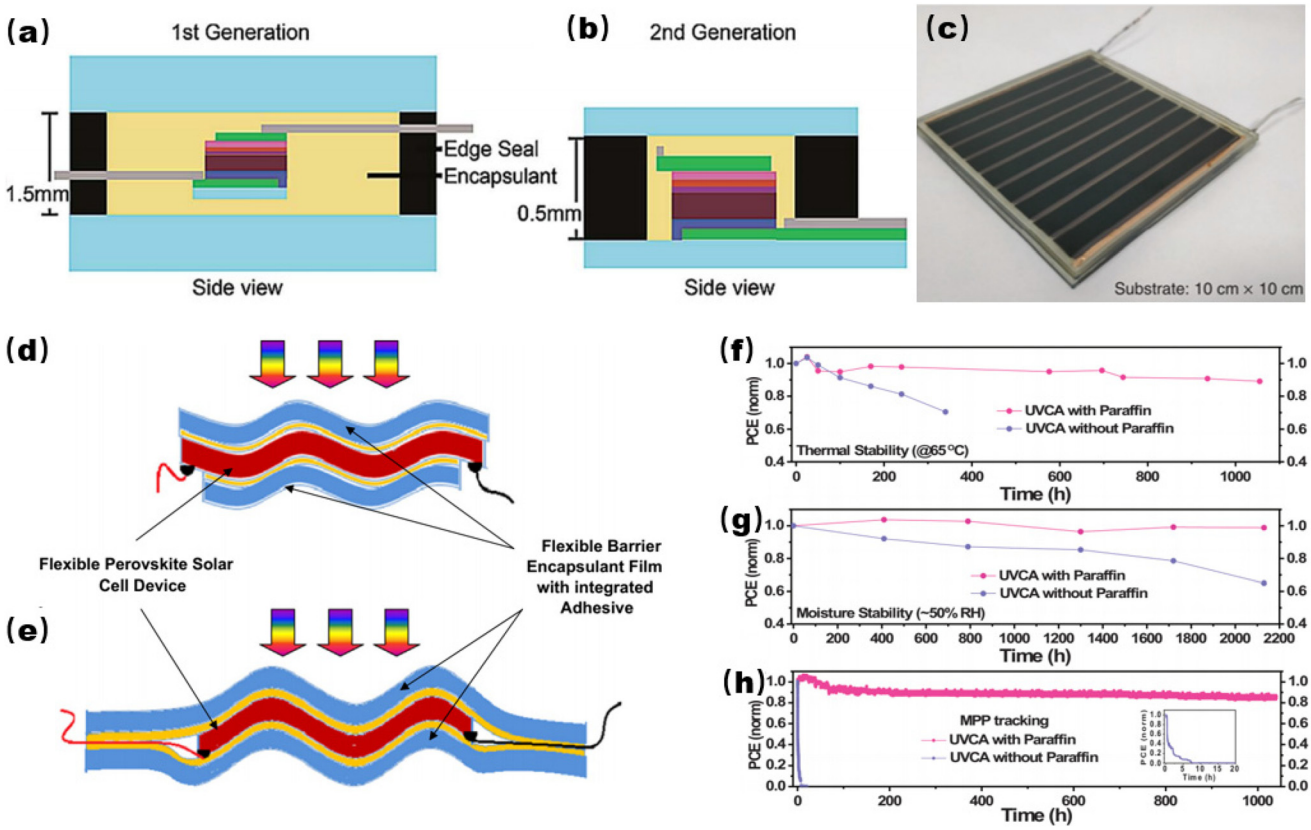

Fig. 8 Side view of (a) first-generation and (b) second-generation package assembly (not to scale). Reproduced with permission.[118] Copyright 2018 The Royal Society of Chemistry. (c) Photograph of a printable perovskite solar submodule (substrate area: 100 cm^2; active area: 60.09 cm^2) encapsulated with a polyurethane film as the encapsulant and a glass sheet as the back cover. Reproduced with permission.[119] Copyright 2019 Wiley-VCH Verlag GmbH & Co. KGaA, Weinheim. Schematic representation of (d) 'partial' and (e) 'complete' encapsulation architectures. Reproduced with permission.[120] Copyright 2015 Elsevier Ltd. (f) Thermal stability and (g) moisture stability tracking of encapsulated devices.[121] (h) Continuous MPP tracking under ambient conditions with different packaging conditions. Inset: the MPP tracking of UVCA without paraffin encapsulation over a short time range. Reproduced with permission.[121] Copyright 2019 Wiley-VCH Verlag GmbH & Co. KGaA, Weinheim.

without paraffin-packaged PSCs are tracked by periodic testing, as shown in Fig. 8f and g. It can be clearly observed that the PSC packaged with UVCA and paraffin exhibits excellent thermal stability, maintaining about 90% of the original PCE after annealing at 65 °C under ambient conditions (40–60% RH) for 1000 h. Meanwhile, the PCE of the UVCA without paraffin-packaged cells decreased rapidly. MPP measurement is now considered to be the most valuable and convincing testing protocol for assessing the stability of the perovskite devices. Fig. 8h shows the MPP tracking of UVCA-encapsulated PSCs with/without paraffin. It can be observed that the UVCA without paraffin-packaged PSC undergoes significant PCE decay, and the PCE device completely degraded within 10 hours due to the presence of moisture and oxygen in the headspace above the PSC. In contrast, the UVCA with paraffin-packaged PSC shows outstanding stability. Even after 1000 h of MPP tracking, the PSC maintained more than 80% of its original efficiency. In summary, device packaging is crucial for the practical operation of the perovskite devices, whereas advanced packaging technologies, such as a solvent-free process and packaging based on an additional functional layer, will help to prepare more stable perovskite devices under various conditions.

4. Conclusion

In summary, the recent fast development of perovskite solar cells was mostly due to the obvious advantageous properties of the metal halide perovskite materials, including tunable band gaps, high absorption coefficients and long carrier diffusion length. In addition, the fundamental understanding on thin-film nucleation and growth kinetics, thermodynamics, colloidal chemistry, advanced thin-film technology, semiconductor doping technology, and interface engineering, has contributed to the rapid progress of PSCs toward improved efficiency, stability and scalability. So far, the PCEs and scalability of PSCs are competitive with conventional solar cells, indicating that PSC is a promising PV technology. However, the instability of the resulting devices is still the biggest obstacle to the industrialization of the perovskite PV technologies. In this review, by learning from the anti-corrosion strat-

Published on 24 mars 2023. Downloaded on 22.06.2024 18.45.27.

egy, we summarized and analyzed existing strategies to improve the lifetimes of the perovskite devices.

(1) Elimination of corrosion sites during fabrication. Variations in the composition and structure of the materials from the precursor to the resulting perovskite will lead to various defects. During long-term operation, these defects often act as initiators of degradation to deteriorate the PSC performance. To eliminate these defects during fabrication, a series of fruitful passivators were developed. The passivators successfully improved carrier extraction, and prevented the escape of halogen anions and organic cations. Also, machining could help to remove defects. Furthermore, strain-release layers were introduced at the perovskite/substrate interface to eliminate defects stemming from residual tensile strain in the perovskite films.

(2) Elimination of corrosion sites during device operation. Given that the perovskite has a soft crystal lattice, a variety of defects will be generated during device operation. Previous studies found that some self-regenerated redox shuttles could be introduced to eliminate illumination-generated I^0 and Pb^0 defect pairs in a sustainable manner through an electron transfer process. Moreover, photoisomeric molecules could be added during the preparation procedure to dynamically eliminate UV-generated defects wherein the photoisomeric molecule played a role in self-healing and activating light-triggered sustainable passivation sites to achieve continuous defect repairs, and eliminate thermally induced defects (such as phase transitions) during operation by re-annealing treatment.

(3) Prevent corrosive media from invading the perovskite. A series of methods have been developed to prevent contact between the corrosive medium and the perovskite. Surface coating of some hydrophobic molecules is a better way to improve the lifetime of devices. Surface covering layers could prevent the escape of halide species and organic cations, inhibit the surface-mediated degradation of perovskites, prevent ion migration induced degradation, and prevent corrosive media from coming in contact with the perovskite. In addition, compact CTMs also act as an effective barrier between the corrosive medium and the perovskite. Furthermore, preventing corrosive media from coming in contact with the perovskite depends on the choice of edge and filling materials and the optimization of packaging techniques.

The aforesaid strategies are found to be fruitful for improving the lifetime of the perovskite devices, but are not enough for the industrialization of PSCs because of the strict stability requirement. To further extend the service lifetime of PSCs up to over 25 years, it is necessary to minimize the corrosion sites and prevent corrosive media from contacting perovskite. Here, we suggested a few research directions with respect to corrosion science, which might serve as powerful solutions to improve the device stability.

(1) Reduce corrosion sites. The following methods are developed to reduce corrosion sites of the perovskite:

(a) Solvent-free techniques. To date, the most commonly used solvents for the fabrication of PSCs with excellent performance are still polar solvents, such as GBL, DMSO, DMF, and/or their mixtures with adjustable coordination ability. However, these highly coordinating solvents will lead to a variety of defects when the bonding solvent evaporates during the annealing process. To thoroughly overcome the solvent-induced defects in the perovskite devices, the development of solvent-free techniques is of great significance. Solvent-free techniques could eliminate defects and random changes to the crystal structure upon going from the precursor to the resulting polycrystalline perovskite.

(b) Dynamic *in-situ* passivation. Defect passivation is considered to be an effective method to realize high performance and stable PSCs. Most passivation strategies are aimed at eliminating defects generated during fabrication. To further develop passivation, we recommend developing some dynamic *in situ* passivation strategies to eliminate newly created surface and bulk defects during device operation. Some redox shuttle or photoisomeric molecules can be added during preparation to achieve a cyclic transition when photoinduced defects appear during subsequent operations.

(c) Non-destructive testing. To date, a thorough understanding of the operational stability of the perovskite devices has been lacking. Common characterization techniques, such as SEM, XRD, and XPS, can cause irreversible damage to the device. Therefore, it is not possible to detect *in situ* states of the same device under different operating conditions. There is an urgent need to develop non-destructive testing technology that can be coupled with stability testing of the perovskite solar cells. Non-destructive testing (NDT) is a testing and analysis technique used in industry to evaluate materials, components, structures or systems for differences in performance or weld defects and discontinuities, without causing damage to the original part. For example, coupling IPCE testing with stability tracking could lead to the identification of different types of defects during device operation through detecting the change of band edges. Coupling an EIS test with a stability test could permit the detection of the interface that generates defects preferentially during subsequent operation. Additionally, coupling PL mapping testing with stability testing could determine if non-radiative recombination preferentially occurred in the bulk or at the interface during operation.

(d) Single-crystal devices. Single crystals have orders of magnitude lower defect densities than polycrystalline thin films. The perovskite films have many grain boundaries, which are the aggregation sites of defects. These defects will eventually result in charge recombination, which affects the device efficiency. Besides, they will become initiation sites for moisture induced degradation and photoinduced ion migration. Therefore, the preparation of single crystal perovskite devices is a significant strategy to reduce corrosion sites.

(2) Barrier protection: A barrier could be constructed between the surface of the perovskite and corrosive medium *via* the following methods:

(a) Exploiting suitable HTM. To further prevent contact between corrosive media and the perovskite, it is crucial to

 This journal is © The Royal Society of Chemistry 2023

Published on 24 mars 2023. Downloaded on 22.06.2024 18.45.27.

develop suitable HTMs with functional groups that can physically protect the perovskite from ion migration induced by light, heat, and bias. HTMs with suitable thermal expansion coefficients should also be considered; these could tune strain in the perovskites and reduce ion mobility.

(b) Encapsulation. Vacuum lamination encapsulation is the most promising technology to prevent corrosive media from coming in contact with the perovskite, but the high-temperature lamination process needs to be improved to be compatible with PSCs. In addition, polymers with strong bonding to lead could be used as lead prevention fillers to further enhance the environmental friendliness of the device.

(3) "Sacrificial Protection". Sacrificial protection is a common corrosion protection strategy in which a more electrochemically active metal is electrically attached to a less active metal. The highly active metal donates electrons to replace those that may have been lost during oxidation of the protected metal. We can improve the stability of PSCs through a similar strategy. For example, in a printable hole-conductor-free mesoscopic device, the perovskite film thickness is as high as 10 μm, and the perovskite in the carbon electrode part serves as the perovskite sacrificial layer, which helps to prolong the life of the device. Sacrificial protection is a promising approach for the industrialization of stable perovskite solar cells, and has been employed in Wonder Solar. However, considering the golden triangle of solar cells based on cost, efficiency and lifetime parameters, it still not clear whether this strategy is the ultimate solution for the industrialization of perovskite solar cells.

In a word, more strategies need to be developed to enhance the lifetime of the perovskite devices, which helps establish a systematic methodology. Just as anticorrosion strategies guide the enhancement of the stability of perovskite devices, newly developed strategies to improve the perovskite stability can also feedback into the anticorrosion field and other fields.

Conflicts of interest

There are no conflicts to declare.

Acknowledgements

The authors acknowledge funding support from the National Natural Science Foundation of China (51972004, 22109002 and 52125206), the National Key Research and Development Program of China (Grant No. 2020YFB1506400), and the Tencent Foundation through the XPLORER PRIZE.

References

1 V. G. Childe, *The Dawn of European Civilization*, Routledge, 2013.
2 G. Basalla, *The Evolution of Technology*, Cambridge University Press, 1988.
3 M. V. Gandhi and B. Thompson, *Smart Materials and Structures*, Springer Science & Business Media, 1992.
4 K. Schwab, *The Fourth Industrial Revolution*, Currency, 2017.
5 A. W. Johnson and T. K. Earle, *The Evolution of Human Societies: from Foraging Group to Agrarian State*, Stanford University Press, 2000.
6 Y. Hassan, J. H. Park, M. L. Crawford, A. Sadhanala, J. Lee, J. C. Sadighian, E. Mosconi, R. Shivanna, E. Radicchi, M. Jeong, C. Yang, H. Choi, S. H. Park, M. H. Song, F. De Angelis, C. Y. Wong, R. H. Friend, B. R. Lee and H. J. Snaith, *Nature*, 2021, **591**, 72–77.
7 J. J. Yoo, G. Seo, M. R. Chua, T. G. Park, Y. Lu, F. Rotermund, Y.-K. Kim, C. S. Moon, N. J. Jeon, J.-P. Correa-Baena, V. Bulović, S. S. Shin, M. G. Bawendi and J. Seo, *Nature*, 2021, **590**, 587–593.
8 H. Min, D. Y. Lee, J. Kim, G. Kim, K. S. Lee, J. Kim, M. J. Paik, Y. K. Kim, K. S. Kim, M. G. Kim, T. J. Shin and S. Il Seok, *Nature*, 2021, **598**, 444–450.
9 Q. Jiang, J. Tong, Y. Xian, R. A. Kerner, S. P. Dunfield, C. Xiao, R. A. Scheidt, D. Kuciauskas, X. Wang, M. P. Hautzinger, R. Tirawat, M. C. Beard, D. P. Fenning, J. J. Berry, B. W. Larson, Y. Yan and K. Zhu, *Nature*, 2022, **611**, 278–283.
10 S. Hu, K. Otsuka, R. Murdey, T. Nakamura, M. A. Truong, T. Yamada, T. Handa, K. Matsuda, K. Nakano, A. Sato, K. Marumoto, K. Tajima, Y. Kanemitsu and A. Wakamiya, *Energy Environ. Sci.*, 2022, **15**, 2096–2107.
11 S. Tao, I. Schmidt, G. Brocks, J. Jiang, I. Tranca, K. Meerholz and S. Olthof, *Nat. Commun.*, 2019, **10**, 2560.
12 Q. Liang, K. Liu, M. Sun, Z. Ren, P. W. K. Fong, J. Huang, M. Qin, Z. Wu, D. Shen, C. S. Lee, J. Hao, X. Lu, B. Huang and G. Li, *Adv. Mater.*, 2022, **34**, 2200276.
13 H. Li, J. Zhou, L. Tan, M. Li, C. Jiang, S. Wang, X. Zhao, Y. Liu, Y. Zhang, Y. Ye, W. Tress and C. Yi, *Sci. Adv.*, 2022, **8**, eabo7422.
14 H.-S. Yun, H. W. Kwon, M. J. Paik, S. Hong, J. Kim, E. Noh, J. Park, Y. Lee and S. Il Seok, *Nat. Energy*, 2022, **7**, 828–834.
15 L. Li, Y. Wang, X. Wang, R. Lin, X. Luo, Z. Liu, K. Zhou, S. Xiong, Q. Bao, G. Chen, Y. Tian, Y. Deng, K. Xiao, J. Wu, M. I. Saidaminov, H. Lin, C.-Q. Ma, Z. Zhao, Y. Wu, L. Zhang and H. Tan, *Nat. Energy*, 2022, **7**, 708–717.
16 Best Research Cell Efficiency Chart. **https://wwwnrelgov/pv/cell-efficiencyhtml**.
17 C. Zheng and O. Rubel, *J. Phys. Chem. C*, 2017, **121**, 11977–11984.
18 N. Aristidou, I. Sanchez-Molina, T. Chotchuangchutchaval, M. Brown, L. Martinez, T. Rath and S. A. Haque, *Angew. Chem., Int. Ed.*, 2015, **54**, 8208–8212.
19 C. C. Boyd, R. Cheacharoen, T. Leijtens and M. D. McGehee, *Chem. Rev.*, 2018, **119**, 3418–3451.
20 Y. Li, X. Xu, C. Wang, B. Ecker, J. Yang, J. Huang and Y. Gao, *J. Phys. Chem. C*, 2017, **121**, 3904–3910.
21 S. Wang, Y. Jiang, E. J. Juarez-Perez, L. K. Ono and Y. Qi, *Nat. Energy*, 2016, **2**, 16195.

Published on 24 mars 2023. Downloaded on 22.06.2024 18.45.27.

22 T. L. Leung, I. Ahmad, A. A. Syed, A. M. C. Ng, J. Popović and A. B. Djurišić, *Commun. Mater.*, 2022, **3**, 63.
23 D. Zhang, D. Li, Y. Hu, A. Mei and H. Han, *Commun. Mater.*, 2022, **3**, 58.
24 G. Zhang, J. Zhang, Z. Yang, Z. Pan, H. Rao and X. Zhong, *Adv. Mater.*, 2022, **34**, 2206222.
25 L. A. Muscarella and B. Ehrler, *Joule*, 2022, **6**, 2016–2031.
26 G. Grancini, C. Roldán-Carmona, I. Zimmermann, E. Mosconi, X. Lee, D. Martineau, S. Narbey, F. Oswald, F. De Angelis, M. Graetzel and M. K. Nazeeruddin, *Nat. Commun.*, 2017, **8**, 15684.
27 R. A. Kerner, Z. Xu, B. W. Larson and B. P. Rand, *Joule*, 2021, **5**, 2273–2295.
28 M. V. Khenkin, E. A. Katz, A. Abate, G. Bardizza, J. J. Berry, C. Brabec, F. Brunetti, V. Bulović, Q. Burlingame, A. Di Carlo, R. Cheacharoen, Y.-B. Cheng, A. Colsmann, S. Cros, K. Domanski, M. Dusza, C. J. Fell, S. R. Forrest, Y. Galagan, D. Di Girolamo, M. Grätzel, A. Hagfeldt, E. von Hauff, H. Hoppe, J. Kettle, H. Köbler, M. S. Leite, S. Liu, Y.-L. Loo, J. M. Luther, C.-Q. Ma, M. Madsen, M. Manceau, M. Matheron, M. McGehee, R. Meitzner, M. K. Nazeeruddin, A. F. Nogueira, Ç. Odabaşı, A. Osherov, N.-G. Park, M. O. Reese, F. De Rossi, M. Saliba, U. S. Schubert, H. J. Snaith, S. D. Stranks, W. Tress, P. A. Troshin, V. Turkovic, S. Veenstra, I. Visoly-Fisher, A. Walsh, T. Watson, H. Xie, R. Yıldırım, S. M. Zakeeruddin, K. Zhu and M. Lira-Cantu, *Nat. Energy*, 2020, **5**, 35–49.
29 T. Wang, Y. Li, Q. Cao, J. Yang, B. Yang, X. Pu, Y. Zhang, J. Zhao, Y. Zhang, H. Chen, A. Hagfeldt and X. Li, *Energy Environ. Sci.*, 2022, **15**, 4414–4424.
30 Y. Niu, Y. Peng, X. Zhang, Y. Ren, R. Ghadari, J. Zhu, G. Tulloch, H. Zhang, P. Falaras and L. Hu, *ACS Energy Lett.*, 2022, **7**, 3104–3111.
31 A. Popoola, O. Olorunniwo and O. Ige, *Dev. Corros. Prot.*, 2014, **13**, 241–270.
32 P. R. Roberge, *Handbook of Corrosion Engineering*, McGraw-Hill Education, 2019.
33 H. A. Videla and L. K. Herrera, *Int. Microbiol.*, 2005, **8**, 169.
34 M. Sharma, H. Jindal, D. Kumar, S. Kumar and R. Kumar, *J. Future Eng. Technol.*, 2021, **17**, 26–36.
35 S. Wieghold, E. M. Cope, G. Moller, N. Shirato, B. Guzelturk, V. Rose and L. Nienhaus, *ACS Energy Lett.*, 2022, **7**, 2211–2218.
36 C.-M. Liao, *Particle-induced Pitting Corrosion of Aluminum Alloys*, Lehigh University, 1998.
37 M. Qin, Y. Li, Y. Yang, P. F. Chan, S. Li, Z. Qin, X. Guo, L. Shu, Y. Zhu, Z. Fan, C.-J. Su and X. Lu, *ACS Energy Lett.*, 2022, **7**, 3251–3259.
38 Z. Zhang, M. A. Kamarudin, A. K. Baranwal, G. Kapil, S. R. Sahamir, Y. Sanehira, M. Chen, L. Wang, Q. Shen and S. Hayase, *Angew. Chem., Int. Ed.*, 2022, **134**, e202210101.
39 G. Liu, Y. Zhong, W. Feng, M. Yang, G. Yang, J. X. Zhong, T. Tian, J. B. Luo, J. Tao, S. Yang, X. D. Wang, L. Tan, Y. Chen and W. Q. Wu, *Angew. Chem., Int. Ed.*, 2022, **134**, e202209464.
40 M. Zhang, T. Li, G. Zheng, L. Li, M. Qin, S. Zhang, H. Zhou and X. Zhan, *Mater. Chem. Front.*, 2017, **1**, 2078–2084.
41 Z. Liu, J. Hu, H. Jiao, L. Li, G. Zheng, Y. Chen, Y. Huang, Q. Zhang, C. Shen, Q. Chen and H. Zhou, *Adv. Mater.*, 2017, **29**, 1606774.
42 Y. Chen, N. Li, L. Wang, L. Li, Z. Xu, H. Jiao, P. Liu, C. Zhu, H. Zai, M. Sun, W. Zou, S. Zhang, G. Xing, X. Liu, J. Wang, D. Li, B. Huang, Q. Chen and H. Zhou, *Nat. Commun.*, 2019, **10**, 1112.
43 S. Chen, Y. Liu, X. Xiao, Z. Yu, Y. Deng, X. Dai, Z. Ni and J. Huang, *Joule*, 2020, **4**, 2661–2674.
44 Y. Z. Lin, Y. Liu, S. S. Chen, S. Wang, Z. Y. Ni, C. H. Van Brackle, S. Yang, J. J. Zhao, Z. H. Yu, X. Z. Dai, Q. Wang, Y. H. Deng and J. S. Huang, *Energy Environ. Sci.*, 2021, **14**, 1563–1572.
45 L. Zhao, Q. Li, C.-H. Hou, S. Li, X. Yang, J. Wu, S. Zhang, Q. Hu, Y. Wang, Y. Zhang, Y. Jiang, S. Jia, J.-J. Shyue, T. P. Russell, Q. Gong, X. Hu and R. Zhu, *J. Am. Chem. Soc.*, 2022, **144**, 1700–1708.
46 S. Liu, X. Guan, W. Xiao, R. Chen, J. Zhou, F. Ren, J. Wang, W. Chen, S. Li, L. Qiu, Y. Zhao, Z. Liu and W. Chen, *Adv. Funct. Mater.*, 2022, **32**, 2205009.
47 J. Tao, X. Liu, J. Shen, S. Han, L. Guan, G. Fu, D.-B. Kuang and S. Yang, *ACS Nano*, 2022, **16**, 10798–10810.
48 Q. Zhou, D. He, Q. Zhuang, B. Liu, R. Li, H. Li, Z. Zhang, H. Yang, P. Zhao, Y. He, Z. Zang and J. Chen, *Adv. Funct. Mater.*, 2022, **32**, 2205507.
49 P. L. Lewis, M. Kolody and J. Curran, *Alternative to Nitric Acid for Passivation of Stainless Steel Alloys*, 2013.
50 D. Yasensky, J. Reali, C. Larson and C. Carl, 2011, Aircraft Airworthiness and Sustainment Conference, 2009.
51 L. R. Jordan, A. J. Betts, K. L. Dahm, P. A. Dearnley and G. A. Wright, *Corros. Sci.*, 2005, **47**, 1085–1096.
52 Y. Wu, Q. Wang, Y. Chen, W. Qiu and Q. Peng, *Energy Environ. Sci.*, 2022, **15**, 4700–4709.
53 Z. Guo, S. Zhao, N. Shibayama, A. K. Jena, I. Takei and T. Miyasaka, *Adv. Funct. Mater.*, 2022, **32**, 2207554.
54 J. Xiong, N. Liu, X. Hu, Y. Qi, W. Liu, J. Dai, Y. Zhang, Z. Dai, X. Zhang, Y. Huang, Z. Zhang, Q. Dai and J. Zhang, *Adv. Energy Mater.*, 2022, **12**, 2201787.
55 K. Zhang, A. Späth, O. Almora, V. M. Le Corre, J. Wortmann, J. Zhang, Z. Xie, A. Barabash, M. S. Hammer, T. Heumüller, J. Min, R. Fink, L. Lüer, N. Li and C. J. Brabec, *ACS Energy Lett.*, 2022, **7**, 3235–3243.
56 M. A. Mahmud, J. Zheng, S. Tang, G. Wang, J. Bing, A. D. Bui, J. Qu, L. Yang, C. Liao, H. Chen, S. P. Bremner, H. T. Nguyen, J. Cairney and A. W. Y. Ho-Baillie, *Adv. Energy Mater.*, 2022, **12**, 2201672.
57 X. Zhang, D. Zhang, Y. Zhou, Y. Du, J. Jin, Z. Zhu, Z. Wang, X. Cui, J. Li, S. Wu, J. Zhang and Q. Tai, *Adv. Funct. Mater.*, 2022, **32**, 2205478.
58 X. Luo, Z. Shen, Y. Shen, Z. Su, X. Gao, Y. Wang, Q. Han and L. Han, *Adv. Mater.*, 2022, **34**, 2202100.

 This journal is © The Royal Society of Chemistry 2023

Published on 24 mars 2023. Downloaded on 22.06.2024 18.45.27.

59 L. Yang, J. Feng, Z. Liu, Y. Duan, S. Zhan, S. Yang, K. He, Y. Li, Y. Zhou, N. Yuan, J. Ding and S. Liu, *Adv. Mater.*, 2022, **34**, 2201681.
60 R. Wang, J. J. Xue, K.-L. Wang, Z.-K. Wang, Y. Q. Luo, D. Fenning, G. W. Xu, S. Nuryyeva, T. Y. Huang, Y. P. Zhao, J. L. Yang, J. H. Zhu, M. H. Wang, S. Tan, I. Yavuz, K. N. Houk and Y. Yang, *Science*, 2019, **366**, 1509–1513.
61 S. Yang, S. Chen, E. Mosconi, Y. Fang, X. Xiao, C. Wang, Y. Zhou, Z. Yu, J. Zhao, Y. Gao, F. De Angelis and J. Huang, *Science*, 2019, **365**, 473–478.
62 X. Li, W. Zhang, X. Guo, C. Lu, J. Wei and J. Fang, *Science*, 2022, **375**, 434–437.
63 S. Tan, T. Huang, I. Yavuz, R. Wang, T. W. Yoon, M. Xu, Q. Xing, K. Park, D.-K. Lee, C.-H. Chen, R. Zheng, T. Yoon, Y. Zhao, H.-C. Wang, D. Meng, J. Xue, Y. J. Song, X. Pan, N.-G. Park, J.-W. Lee and Y. Yang, *Nature*, 2022, **605**, 268–273.
64 N. Li, S. Tao, Y. Chen, X. Niu, C. K. Onwudinanti, C. Hu, Z. Qiu, Z. Xu, G. Zheng, L. Wang, Y. Zhang, L. Li, H. Liu, Y. Lun, J. Hong, X. Wang, Y. Liu, H. Xie, Y. Gao, Y. Bai, S. Yang, G. Brocks, Q. Chen and H. Zhou, *Nat. Energy*, 2019, **4**, 408–415.
65 X. Zheng, B. Chen, J. Dai, Y. Fang, Y. Bai, Y. Lin, H. Wei, X. C. Zeng and J. Huang, *Nat. Energy*, 2017, **2**, 17102.
66 Y. Guo, S. Apergi, N. Li, M. Chen, C. Yin, Z. Yuan, F. Gao, F. Xie, G. Brocks, S. Tao and N. Zhao, *Nat. Commun.*, 2021, **12**, 644.
67 R. Lin, J. Xu, M. Wei, Y. Wang, Z. Qin, Z. Liu, J. Wu, K. Xiao, B. Chen, S. M. Park, G. Chen, H. R. Atapattu, K. R. Graham, J. Xu, J. Zhu, L. Li, C. Zhang, E. H. Sargent and H. Tan, *Nature*, 2022, **603**, 73–78.
68 M. Scardamaglia, V. Boix, G. D'Acunto, C. Struzzi, N. Reckinger, X. Chen, A. Shivayogimath, T. Booth and J. Knudsen, *Carbon*, 2021, **171**, 610–617.
69 L. Shen, Y. Zhao, Y. Wang, R. Song, Q. Yao, S. Chen and Y. Chai, *J. Mater. Chem. A*, 2016, **4**, 5044–5050.
70 L. Camilli, F. Yu, A. Cassidy, L. Hornekær and P. Bøggild, *2D Mater.*, 2019, **6**, 022002.
71 M. Scardamaglia, C. Struzzi, A. Zakharov, N. Reckinger, P. Zeller, M. Amati and L. Gregoratti, *ACS Appl. Mater. Interfaces*, 2019, **11**, 29448–29457.
72 S. Jia, W. Chen, J. Zhang, C. Y. Lin, H. Guo, G. Lu, K. Li, T. Zhai, Q. Ai and J. Lou, *Mater. Today Nano*, 2021, **16**, 100135.
73 Z. Liu, Y. Gong, W. Zhou, L. Ma, J. Yu, J. C. Idrobo, J. Jung, A. H. MacDonald, R. Vajtai, J. Lou and P. M. Ajayan, *Nat. Commun.*, 2013, **4**, 2541.
74 S. Böhm, *Nat. Nanotechnol.*, 2014, **9**, 741–742.
75 R. S. Weatherup, L. D'Arsié, A. Cabrero-Vilatela, S. Caneva, R. Blume, J. Robertson, R. Schloegl and S. Hofmann, *J. Am. Chem. Soc.*, 2015, **137**, 14358–14366.
76 E. H. Jung, N. J. Jeon, E. Y. Park, C. S. Moon, T. J. Shin, T.-Y. Yang, J. H. Noh and J. Seo, *Nature*, 2019, **567**, 511–515.
77 S. Yang, Y. Wang, P. Liu, Y.-B. Cheng, H. J. Zhao and H. G. Yang, *Nat. Energy*, 2016, **1**, 15016.
78 R. Azmi, E. Ugur, A. Seitkhan, F. Aljamaan, A. S. Subbiah, J. Liu, G. T. Harrison, M. I. Nugraha, M. K. Eswaran, M. Babics, Y. Chen, F. Xu, T. G. Allen, A. u. Rehman, C.-L. Wang, T. D. Anthopoulos, U. Schwingenschlögl, M. De Bastiani, E. Aydin and S. De Wolf, *Science*, 2022, **376**, 73–77.
79 F. Zhang, S. Y. Park, C. L. Yao, H. P. Lu, S. P. Dunfield, C. X. Xiao, S. Uličná, X. M. Zhao, L. Du Hill, X. H. Chen, X. M. Wang, L. E. Mundt, K. H. Stone, L. T. Schelhas, G. Teeter, S. Parkin, E. L. Ratcliff, Y. L. Loo, J. J. Berry, M. C. Beard, Y. F. Yan, B. W. Larson and K. Zhu, *Science*, 2022, **375**, 71–76.
80 X. Zhao, T. Liu, Q. C. Burlingame, T. Liu, R. Holley III, G. Cheng, N. Yao, F. Gao and Y.-L. Loo, *Science*, 2022, **377**, 307–310.
81 Y. Wang, T. Wu, J. Barbaud, W. Kong, D. Cui, H. Chen, X. Yang and L. Han, *Science*, 2019, **365**, 687–691.
82 L. Yang, Q. Xiong, Y. Li, P. Gao, B. Xu, H. Lin, X. Li and T. Miyasaka, *J. Mater. Chem. A*, 2021, **9**, 1574–1582.
83 M. Uddin, H. Rosman, C. Hall and P. Murphy, *Int. J. Adv. Manuf. Technol.*, 2017, **90**, 2095–2108.
84 J. Yu, M. Wang and S. Lin, *ACS Nano*, 2016, **10**, 11044–11057.
85 C. Stavrakas, S. J. Zelewski, K. Frohna, E. P. Booker, K. Galkowski, K. Ji, E. Ruggeri, S. Mackowski, R. Kudrawiec, P. Plochocka and S. D. Stranks, *Adv. Energy Mater.*, 2019, **9**, 1901883.
86 3M. 3MTMTemflexTM Vinyl Electrical Tape 1700. **https://www.3m.com/3M/en_US/company-us/all-3m-products/~/3M-Temflex-Vinyl-Electrical-Tape-1700/?N=5002385+3294355723&rt=rud**.
87 E. J. Juarez-Perez, Z. Hawash, S. R. Raga, L. K. Ono and Y. Qi, *Energy Environ. Sci.*, 2016, **9**, 3406–3410.
88 E. J. Juarez-Perez, L. K. Ono, I. Uriarte, E. J. Cocinero and Y. Qi, *ACS Appl. Mater. Interfaces*, 2019, **11**, 12586–12593.
89 C. A. Loto, *Int. J. Adv. Manuf. Technol.*, 2017, **93**, 3567–3582.
90 H. Zhang and N.-G. Park, *Angew. Chem., Int. Ed.*, 2022, **61**, e202212268.
91 W. Meng, K. Zhang, A. Osvet, J. Zhang, W. Gruber, K. Forberich, B. Meyer, W. Heiss, T. Unruh, N. Li and C. J. Brabec, *Joule*, 2022, **6**, 458–475.
92 D.-J. Xue, Y. Hou, S.-C. Liu, M. Wei, B. Chen, Z. Huang, Z. Li, B. Sun, A. H. Proppe, Y. Dong, M. I. Saidaminov, S. O. Kelley, J.-S. Hu and E. H. Sargent, *Nat. Commun.*, 2020, **11**, 1514.
93 C. Ge, M. Hu, P. Wu, Q. Tan, Z. Chen, Y. Wang, J. Shi and J. Feng, *J. Phys. Chem. C*, 2018, **122**, 15973–15978.
94 M. Keshavarz, M. Ottesen, S. Wiedmann, M. Wharmby, R. Küchler, H. Yuan, E. Debroye, J. A. Steele, J. Martens, N. E. Hussey, M. Bremholm, M. B. J. Roeffaers and J. Hofkens, *Adv. Mater.*, 2019, **31**, 1900521.
95 T. J. Jacobsson, L. J. Schwan, M. Ottosson, A. Hagfeldt and T. Edvinsson, *Inorg. Chem.*, 2015, **54**, 10678–10685.
96 T. Burwig, W. Fränzel and P. Pistor, *J. Phys. Chem. Lett.*, 2018, **9**, 4808–4813.

Published on 24 mars 2023. Downloaded on 22.06.2024 18.45.27.

97 N. Rolston, K. A. Bush, A. D. Printz, A. Gold-Parker, Y. Ding, M. F. Toney, M. D. McGehee and R. H. Dauskardt, *Adv. Energy Mater.*, 2018, **8**, 1802139.
98 J. Zhao, Y. Deng, H. Wei, X. Zheng, Z. Yu, Y. Shao, J. E. Shield and J. Huang, *Sci. Adv.*, 2017, **3**, eaao5616.
99 H. Wang, C. Zhu, L. Liu, S. Ma, P. Liu, J. Wu, C. Shi, Q. Du, Y. Hao, S. Xiang, H. Chen, P. Chen, Y. Bai, H. Zhou, Y. Li and Q. Chen, *Adv. Mater.*, 2019, **31**, 1904408.
100 T. Liu, X. Zhao, X. Zhong, Q. C. Burlingame, A. Kahn and Y.-L. Loo, *ACS Energy Lett.*, 2022, **7**, 3531–3538.
101 S. R. Raga, M.-C. Jung, M. V. Lee, M. R. Leyden, Y. Kato and Y. Qi, *Chem. Mater.*, 2015, **27**, 1597–1603.
102 B. Philippe, T. J. Jacobsson, J.-P. Correa-Baena, N. K. Jena, A. Banerjee, S. Chakraborty, U. B. Cappel, R. Ahuja, A. Hagfeldt, M. Odelius and H. Rensmo, *J. Phys. Chem. C*, 2017, **121**, 26655–26666.
103 H. Cho, S.-H. Jeong, M.-H. Park, Y.-H. Kim, C. Wolf, C.-L. Lee, J. H. Heo, A. Sadhanala, N. Myoung, S. Yoo, S. H. Im, R. H. Friend and T.-W. Lee, *Science*, 2015, **350**, 1222–1225.
104 L. Wang, H. Zhou, J. Hu, B. Huang, M. Sun, B. Dong, G. Zheng, Y. Huang, Y. Chen and L. Li, *Science*, 2019, **363**, 265–270.
105 Y. Wang, H. Yang, K. Zhang, M. Tao, M. Li and Y. Song, *ACS Energy Lett.*, 2022, **7**, 3646–3652.
106 Y. R. Shi, K. L. Wang, Y. H. Lou, G. L. Liu, C. H. Chen, J. Chen, L. Zhang and Z. K. Wang, *Adv. Mater.*, 2022, **34**, 2205338.
107 H. Liu, N. Li, Z. Chen, S. Tao, C. Li, L. Jiang, X. Niu, Q. Chen, F. Wang, Y. Zhang, Z. Huang, T. Song and H. Zhou, *Adv. Mater.*, 2022, **34**, 2204458.
108 G. Cui, Z. Bi, R. Zhang, J. Liu, X. Yu and Z. Li, *Chem. Eng. J.*, 2019, **373**, 104–121.
109 N. Liu, Q. Du, G. Yin, P. Liu, L. Li, H. Xie, C. Zhu, Y. Li, H. Zhou, W.-B. Zhang and Q. Chen, *J. Mater. Chem. A*, 2018, **6**, 6806–6814.
110 L. Li, X. Jin, N. Liu, Q. Chen, W.-B. Zhang and H. Zhou, *Sol. RRL*, 2018, **2**, 1800069.
111 S.-H. Turren-Cruz, A. Hagfeldt and M. Saliba, *Science*, 2018, **362**, 449–453.
112 M. Kim, S. G. Motti, R. Sorrentino and A. Petrozza, *Energy Environ. Sci.*, 2018, **11**, 2609–2619.
113 C. Ma and N.-G. Park, *ACS Energy Lett.*, 2020, **5**, 3268–3275.
114 I. Lee, J. H. Yun, H. J. Son and T.-S. Kim, *ACS Appl. Mater. Interfaces*, 2017, **9**, 7029–7035.
115 M. J. Jeong, K. M. Yeom, S. J. Kim, E. H. Jung and J. H. Noh, *Energy Environ. Sci.*, 2021, **14**, 2419–2428.
116 X. Niu, N. Li, C. Zhu, L. Liu, Y. Zhao, Y. Ge, Y. Chen, Z. Xu, Y. Lu, M. Sui, Y. Li, A. Tarasov, E. A. Goodilin, H. Zhou and Q. Chen, *J. Mater. Chem. A*, 2019, **7**, 7338–7346.
117 T. Yoon, W. C. Shin, T. Y. Kim, J. H. Mun, T.-S. Kim and B. J. Cho, *Nano Lett.*, 2012, **12**, 1448–1452.
118 R. Cheacharoen, C. C. Boyd, G. F. Burkhard, T. Leijtens, J. A. Raiford, K. A. Bush, S. F. Bent and M. D. McGehee, *Sustainable Energy Fuels*, 2018, **2**, 2398–2406.
119 Z. Fu, M. Xu, Y. Sheng, Z. Yan, J. Meng, C. Tong, D. Li, Z. Wan, Y. Ming, A. Mei, Y. Hu, Y. Rong and H. Han, *Adv. Funct. Mater.*, 2019, **29**, 1809129.
120 H. C. Weerasinghe, Y. Dkhissi, A. D. Scully, R. A. Caruso and Y.-B. Cheng, *Nano Energy*, 2015, **18**, 118–125.
121 S. Ma, Y. Bai, H. Wang, H. Zai, J. Wu, L. Li, S. Xiang, N. Liu, L. Liu, C. Zhu, G. Liu, X. Niu, H. Chen, H. Zhou, Y. Li and Q. Chen, *Adv. Energy Mater.*, 2020, **10**, 1902472.

This journal is © The Royal Society of Chemistry 2023